Author Manuscript

Author Manuscript

Author Manuscript

Author Manuscript

HHS Public Access

Author manuscript

Biomaterials. Author manuscript; available in PMC 2020 April 01.

Published in final edited form as:

Biomaterials. 2019 April ; 198: 204–216. doi:10.1016/j.biomaterials.2018.08.006.

Multiscale Bioprinting of Vascularized Models

Amir K. Miri[#a,b,c,**], **Akbar Khalilpour**[#a,b], **Berivan Cecen**[#a,b], **Sushila Maharjan**[#a,b], **Su-Ryon Shin**[a,b], and **Ali Khademhosseini**[a,b,d,e,f,g,h,i,**]

[a]Division of Engineering in Medicine, Department of Medicine, Brigham and Women's Hospital, Harvard Medical School, Cambridge, MA 02139, USA

[b]Harvard–MIT Division of Health Sciences and Technology, Cambridge, MA 02139, USA

[c]Department of Mechanical Engineering, Rowan University, Glassboro, NJ 08028, USA

[d]Department of Bioengineering, Department of Chemical and Biomolecular Engineering, Henry Samueli School of Engineering and Applied Sciences, University of California-Los Angeles, Los Angeles, CA, USA

[e]Department of Radiology, David Geffen School of Medicine, University of California-Los Angeles, Los Angeles, CA, USA

[f]Center for Minimally Invasive Therapeutics (C-MIT), University of California-Los Angeles, Los Angeles, CA, USA

[g]California NanoSystems Institute (CNSI), University of California-Los Angeles, Los Angeles, CA, USA

[h]Department of Bioindustrial Technologies, College of Animal Bioscience and Technology, Konkuk University, Seoul, Republic of Korea

[i]Center for Nanotechnology, King Abdulaziz University, Jeddah 21569, Saudi Arabia

[#] These authors contributed equally to this work.

Abstract

A basic prerequisite for the survival and function of three-dimensional (3D) engineered tissue constructs is the establishment of blood vessels. 3D bioprinting of vascular networks with hierarchical structures that resemble *in vivo* structures has allowed blood circulation within thick tissue constructs to accelerate vascularization and enhance tissue regeneration. Successful rapid vascularization of tissue constructs requires synergy between fabrication of perfusable channels and functional bioinks that induce angiogenesis and capillary formation within constructs. Combinations of 3D bioprinting techniques and four-dimensional (4D) printing concepts through patterning proangiogenic factors may offer novel solutions for implantation of thick constructs. In

[**] *Corresponding authors:* Amir K. Miri, PhD, miri@rowan.edu, Ali Khademhosseini, PhD, 5531 Boelter Hall, 4121D Engineering V, Chemical and Biomolecular Engineering Department, Los Angeles, CA 90095, Tel: (310) 206-5819, Fax: (310) 794-5956, khademh@ucla.edu.

Publisher's Disclaimer: This is a PDF file of an unedited manuscript that has been accepted for publication. As a service to our customers we are providing this early version of the manuscript. The manuscript will undergo copyediting, typesetting, and review of the resulting proof before it is published in its final citable form. Please note that during the production process errors may be discovered which could affect the content, and all legal disclaimers that apply to the journal pertain.

Author Manuscript Author Manuscript Author Manuscript Author Manuscript

this review, we cover current bioprinting techniques for vascularized tissue constructs with vasculatures ranging from capillaries to large blood vessels and discuss how to implement these approaches for patterning proangiogenic factors to maintain long-term, stimuli-controlled formation of new capillaries.

Keywords

tissue engineering; sacrificial bioink; core/shell; stereolithography; angiogenesis

1. Introduction

The engineered tissue constructs consist of self-assembled cell aggregates, synthetic materials, biological scaffolds, or porous hydrogels and fibrous meshes with macroscale characteristics that promote cell adhesion, migration, and proliferation [1]. The balance of migration and proliferation of encapsulated cells over their life cycles requires consistent delivery of nutrients and oxygen [2], in particular when constructs implanted for ischemic heart disease [3] and diabetic ulcers [4]. It is thus important to create functional blood vessel networks ranging from a few micrometers to millimeters within complex structures, such as liver, kidney, and heart [5, 6] (Fig. 1). Vascular systems *in vivo* include a mixture of different cell types that undergo continuous remodeling by stimuli from endothelial, nervous, immune, and endocrine cells [7]. They also play a key role in graft perfusion and integration of implants into the host vascular system [8, 9]. Vascular growth is further associated with developmental processes of angiogenesis, wound healing, and the progression of various pathologies such as cancer [9, 10]. Despite significant improvements of current technologies to create three-dimensional (3D) blood vessels, the formation of a functional engineered vascular system with multiscale vessel networks from capillaries to large vessels has remained challenging in this field [11]. Inability in fabrication of 3D vascular networks has limited tissue engineering in the growth of thick tissue or organ-level constructs.

Many approaches have been proposed to induce the growth of a vascular system within 3D engineered tissue constructs [12]. Vascularization has been induced within tissue constructs by incorporation of growth factors into the construct [12] (which yields vasculogenesis), seeding endothelial cells in the construct to stimulate angiogenesis [13], or engineering multiscale microfluidic channels inside biocompatible materials using various microfabrication technologies [14]. Either naturally- or synthetically-derived scaffolds when mixed with proangiogenic factors yield *de novo* formation of capillaries [15]. In another strategy, co-cultures of endothelial cells and other cell types of the desired organ were used within tissue scaffolds prior to their implantation [16]. This strategy depends on the biological properties of endothelial cells to promote the formation of neo-capillaries *in vivo*. Such process can be described by remodeling phenomenon driven by the endothelial cells that are activated by the proangiogenic agents [17]. For example, in the case of human umbilical vein endothelial cell (HUVEC)-loaded collagen hydrogel implant, a tree-like structure of branched capillaries was observed over two months of implantation [17]. Several other studies have shown the ability of endothelial cells along with mesenchymal stem cells (MSCs) to form a stable vascular system under both *in vitro* and *in vivo* conditions [18, 19].

Author Manuscript Author Manuscript Author Manuscript Author Manuscript

In addition to these strategies, microfabrication techniques have been developed to generate perfusable channels in hydrogels [20–22]. Similarly, pre-implant fabrication of capillary networks into tissues constructs has shown accelerated implant integration into the host tissue as well as the formation of capillary-like structures coupled with the host vasculature [23, 24]. However, these approaches lack the ability to directly generate multiscale vessel networks along with anastomosis in the host tissue, which is one of the major challenges in tissue integration.

Conventional engineering of vascular tubes includes sheet rolling and tubular molding [25]. In sheet rolling, a sheet of cellular or acellular biomaterials is rolled over a predefined mandrel and it remodels to a stable and homogeneous structure [26]. The tubular molding can also be used to shape injected biomaterials and crosslink or solidify the tube inside the annular mold [27]. These fabrication methods lack proper control on the structure and are limited to mesoscale blood vessel size (Fig. 1). Recent advancements in materials engineering and microfabrication techniques have further led to the development of new strategies [11] that offer precise control over various aspects of the cell-laden tissue implants including cell patterning [28], cell phenotype [29], cellular alignment [30], as well as the microenvironmental cues including mechanical properties [6], chemical properties (e.g. ligand density), and topographic features (e.g. cell adhesiveness) [9]. Such manipulations along with the use of 3D bioprinting techniques have been successfully applied to overcome the technical challenges of fabricating a functional microvasculature (as shown in Fig. 1 and summarized in Table 1) [6]. Bioprinting has become an essential tool for fabricating vascularized tissue constructs, in which the design of printable, tunable and biocompatible bioink is essential [9, 31]. Common examples of bioink with proper biophysical properties and endogenous cellular cues are alginate [31, 32] and gelatin methacryloyl (GelMA) hydrogels [33–36]. In addition, integration of *time* into bioprinting process known as four-dimensional (4D) bioprinting yields variations in configurational and/or biophysical characteristics of tissue constructs in response to environmental stimuli, which lead to a more realistic formation of capillaries [37]. In this review, we summarize recent 3D bioprinting techniques including sacrificial, core/shell bioprinting techniques and innovations in bioprinting approaches such as 4D bioprinting for making vascularized tissue constructs [9, 11]. We then discuss how nanotechnology can be integrated into the fabrication process to advance delivery of proangiogenic factors and therapeutic compounds. Temporal controls over distributions of neo-capillaries within pre-vascularized implants may solve existing challenges in cell encapsulation of thick tissue constructs, while the designed vasculature can help anastomosis after implantation. Such vascularized models can be designed to deliver therapeutic molecules into the body circulation in a controlled fashion.

2. Sacrificial Bioprinting

Classical bioprinting techniques include active printing of cellular and extracellular components in a predefined shape. Such approaches require rapid gelation or crosslinking process to provide a stable hollow tube construct [9, 38]. To overcome challenges associated with printability of hydrogels and the lack of structural support in fabricating hollow tube constructs, researchers print sacrificial channels that are supported by surrounding walls and then dissolve the channels, known as sacrificial bioprinting. In such a case, vascular network

Author Manuscript Author Manuscript Author Manuscript Author Manuscript

is filled by a fugitive bioink that can be removed by temperature variations or appropriate solvents leaving perfusable channels behind. Materials with reversible crosslinking mechanisms are frequently employed as the fugitive bioink, such as Pluronic F127, agarose, and gelatin. The sacrificial bioprinting approaches have led to the creation of 3D vascularized tissues with robust structural and functional integrity [9, 39]. We have categorized the various sacrificial bioprinting strategies such as extrusion-, inkjet- and light-assisted bioprinting.

2.1 Extrusion-assisted techniques

In the most common case of sacrificial bioprinting, the sacrificial channels loaded by therapeutic agents and cellular components are extruded through a printhead (Fig. 2). The sacrificial channels are then dissolved through thermal modifications, such as melting thermosensitive hydrogels under biological temperature, or chemical reactions, such as enzymatic degradation of protein-based hydrogels, resulting in perfusable vasculature obtained [37, 40]. The surrounding constructs that consist of acrylate-modified hydrogels, such as GelMA, and naturally-derived hydrogels, such as collagen and fibrin, allow cell infiltration into channels, ranging from micrometers to millimeters [9, 39, 41, 42]. Sacrificial extrusion was introduced by agarose as the template of perfusable vessels, from 50 μm to 100 μm in wall thickness and from 800 μm to 2 mm in inner diameter (Fig. 2A). Agarose channels were created within cell-laden GelMA hydrogels that allowed enhanced mass transport in relatively thick hydrogels and yielded proper cellular viability over time, and supported rapid formation of endothelial monolayers [33]. Although this approach is simple and effective, the physical properties of agarose gels hamper the printing resolution (Fig. 2B).

A widely used sacrificial bioink is Pluronic F127, a thermosensitive and shear thinning polymer that melts at 4°C and softens at high shear rates [43]. In addition to biocompatibility and biodegradability, Pluronic F127 has shown great printability for volume fractions higher than 20% v/v in water [34, 44]. For example, vascular channels ranging from 150 μm to 500 μm were created within collagen precursor or a composite of Matrigel® and poly (lactic-co-glycolic) acid (PLGA) for long-term perfusion [37, 45, 46] (Fig. 2C). Kolesky *et al.* co-printed Pluronic F127 mixed with thrombin and HUVEC-laden GelMA vessels using a customized extrusion 3D printer, while the cell encapsulated GelMA hydrogel was crosslinked by UV light to form the surrounding matrix [34]. The printed construct was covered by a cell-free gelatin-fibrinogen bioink, which was loaded by transglutaminase and thrombin for improved crosslinking of remained gelatin and fibrinogen. Homan *et al.* fabricated kidney proximal tubule-on-a-chip by sacrificial bioprinting of Pluronic channels in diameters ranging from 400 μm to 550 μm [47]. They filled the chip by a fibrinogen-gelatin-$CaCl_2$-transglutaminase bioink loaded by fibroblasts and perfused the culture medium to wash out the scarifial channel. The chip when seeded by epithelial cells showed good stability up to two weeks. Wu *et al.* used Pluronic F127 filaments to create vascular networks with diameters ranging from 100 μm to 800 μm within heterogeneous tissue constructs larger than 1 cm thickness and 10 cm^3 volume [46]. However, there have been some drawbacks with Pluronic F127, such as weak stability, low

Author Manuscript Author Manuscript Author Manuscript Author Manuscript

strength, fast degradation, and slow gelation, which have limited its application in tissue engineering [46].

Thermosensitive gelatin hydrogels have also been used extensively as the sacrificial material to create the vascular channels. Vascular channels within a 3D matrix were fabricated by a mixture of fibrinogen, gelatin, thrombin, and cellular components. After incubation at 37°C, an external pump was used to perfuse through 400-μm gelatin channels while endothelial cells became confluent and migrated into the matrix up to 5 mm distance from the channel under physiological flow conditions [6] (Fig. 2D). In a similar work, a single channel was fabricated by bioprinting gelatin channels within collagen sheets and enclosed in a fluidic chip [48]. This chis design was then modified by a two-channel fibrin block loaded by HUVECs for mimicking angiogenic sprouting [45]. Another research group deposited collagen-based layers around gelatin channels containing HUVECs, showing good angiogenesis [49].

In a different material system, carbohydrate glass fibers were adapted as a sacrificed 3D pattern for vascularization [50, 51]. Miller *et al.* extruded melting sucrose-glucose containing dextran to form a 3D glass cage skeleton [50]. This skeleton was buried in cell-laden matrices, followed by molding the matrices and submerging into culture media to form channel nets. These channels, from 150 μm to 750 μm in diameter, were seeded by endothelial cells and conditioned by dynamic flow (Fig. 2E). In contrast to high biocompatibility of this material system, its significant melting temperature (i.e., 80–120°C) prevents the encapsulation of any cellular or protein component.

Recently, freeform reversible embedding of suspended hydrogel was developed for bioprinting of 3D constructs, in which bioink can be deposited with weight support from surrounding granular dense bath made by a thermo-reversible hydrogel [40]. The bath support preserves the structure during bioprinting process and improves geometric fidelity. In addition, embedded bioprinting has enabled the direct 3D printing of biologically relevant bioinks including alginate, collagen type-I precursor, fibrin, and Matrigel® within a sacrificial support bath intended to be removed subsequently [40]. This technique has been used to fabricate vascular network made by deposition of hydrogels in embedded bioprinting.

In summary, sacrificial extrusion-assisted bioprinting of vascularized networks has benefited from great advances in creating multiscale channels with high fidelity and proper biocompatibility. Depending on the nozzle size and printability of bioink, a wide range of channel sizes could be achieved. Among different bioinks, thermosensitive polymers are very promising for fabricating cell-laden vascular constructs. However, the current literature suffers from proper characterization of bioink composition and processing parameters (i.e., pressure, light exposure, etc.) on the biological properties of printed constructs.

2.2 Inkjet-assisted techniques

Inkjet-assisted bioprinting is a fast fabrication process that deposits droplets of bioink onto a hydrogel substrate or culture dish. Among different types of inkjet-assisted bioprinting, thermal and piezoelectric actuation mechanisms have been broadly used [52]. In thermal

Author Manuscript Author Manuscript Author Manuscript Author Manuscript

inkjet bioprinting, bioink droplets are generated by heating [29], whereas in piezoelectric inkjet bioprinting, drops are generated by transient pressure waves from piezoelectric actuator [53]. Nakamura *et al.* have developed an alginate-based bioink with sudden gelation by dipping the inkjet fluid into a calcium chloride (CaCl2) solution to form micro-gel droplets as building blocks [54]. This led to the production of a cell compatible alginate hydrogel container demonstrating 200-μm channels, in one-to-one correlation with the computer-generated images [54, 55]. Later, Pataky *et al.* printed alginate-based bioink into a decellularized and bifurcating vein with a diameter of 200 μm [56]. In addition, thrombin-calcium-based bioink was deposited on a fibrinogen surface to reproduce the intrinsic solidifying process in wound healing [57]. This work led to a dry inkjet printing method with biomimetic gelling *in situ*. Fibrinogen, printed by inkjet printing, showed explosive pressure forces, which are allowed for two-dimensional (2D) cellular microvascular modeling and stable channel formation within 21 days [57] (Fig. 3B).

Similarly, droplet-based bioprinting (DBB) can be used for sacrificial bioprinting of channels [42]. DBB benefits from practical simplicity and swiftness while having precise control on deposition of cells, growth factors, drugs, and therapeutic reagents [37]. In DBB, the artificial cylinder is deposited in a dispenser to form cylindrical shapes, followed by bioprinting of hydrogel layers. The artificial material is then obtained by lining the endothelial cells within the vascularization channels while being liquefied by thermal dissolution. Lee *et al.* demonstrated this concept by creating perfusable vascular channels using an electromechanical microvalve bioprinting technique [45]. This microvalve consisted of a solenoid coil and a piston that can open or close by on/off command. The smallest droplet size was 100 nm, but was used to print fluidic channels with 0.7–1.5 mm width and 0.5–1.2 mm height. Despite several advantages such as rapid deposition, low cost, and high resolution, inkjet-assisted bioprinting has been limited to thin constructs (i.e., a few layers) due to instability of printed layers [52, 59].

2.3 Light-assisted techniques

Light-assisted bioprinting technologies are known as precise, high-resolution fabrication methods to create various constructs. In one approach, laser-assisted printing technology involves an energy absorbing metal layer that generates a high pressure bubble to push the bioink towards a substrate and a pulsed laser beam focused on a strip made from a biological layer [58, 60] (Fig. 3C–D). For vascularized constructs, this approach has been used for the sequential printing of HUVECs and smooth muscle cells into a 2D configuration of branched structures [61]. In general, laser-based manufacturing is limited to 2D applications; however, high cell density printing and single layers can be useful in combinatorial methods for nearly-3D bioprinting by creating multilayers with organizational control [62, 63].

Dynamic digital patterning with digital micro-mirror device (DMD)-based stereolithography systems provide rapid fabrication of 3D constructs at high spatial resolutions (Fig. 3C). Biodegradable, photo-curable polymeric bioinks are commonly used in this technique [64]. The advantage of DMD-based bioprinting systems is superior resolution and fast fabrication time [58, 64]. This technique allows the assembly of highly specified complex hydrogels with micrometer resolutions [65]. Chen *et al.* fabricated 3D tissue constructs of reticular

Author Manuscript Author Manuscript Author Manuscript Author Manuscript

shapes and embedded channels by combinations of GelMA hydrogel and various cell types including fibroblasts, myoblasts endothelial cells, cardiac stem cells, and HUVECs [58, 65]. The addition of methacrylate groups to hyaluronic acid makes it photocrosslinkable while maintaining the biological activity of hyaluronic acid to promote angiogenesis. A multiscale capillary structure, ranging from 100 μm to 1 mm, was fabricated by DMD-based bioprinting system of hyaluronic acid and gelatin as the sacrificial material in GelMA-polyethylene glycol (PEG) medium. To evaluate tissue regeneration ability, the multiscale capillary structure was implanted in a subcutaneous rat model and anastomosis between the grafted implants and the host vasculature was observed after two weeks of implantation [16] (Fig. 3D). Such techniques allow engineering complex tissues, such as liver and tumor tissues [66].

3. Core/Shell Bioprinting

3.1 Alginate-based bioprinting

Among various bioprinting strategies, core/shell geometry seems efficient and promising in creating vascular networks (Fig. 4 A, B) [67]. The main benefit of the core/shell structure is the capacity of fabricating hierarchical, multi-layer tissue constructs with desirable biological and mechanical properties [67]. As a low-cost material, numerous bioengineers employ alginate hydrogel as a component in the design and fabrication of bioinks. Alginate is a naturally occurring, nontoxic, biodegradable and non-immunogenic linear polysaccharide composed of glucuronic and mannuronic acids [68]. Native alginate has no cell-adhesive moieties and shows partial biodegradation. Alginate-based bioinks when used as a matrix scaffold showed cell growth in 3D constructs [31]. The most widely used approaches for alginate-based bioinks are extrusion-assisted bioprinting and inkjet-assisted bioprinting techniques (Fig 4C). Lee and Mooney have indicated that chemical alteration of alginate during oxidation with sodium periodate leads to a controlled rate of degradation [69]. For the reason of this enviable feature for tissue engineering applications, oxidized alginate has promising outlook as a bioink. In another study, alginate hydrogels with diverse oxidation percentages and their concentrations were used to develop a tunable bioink that its material properties can be tailored for a wide range of applications in tissue engineering [31]. The effects of viscosity and mass concentration on the printability of alginate hydrogels were thoroughly studied, and suitable ranges of alginate viscosities and concentrations were proposed for bioink development [31]. Moreover, alginate-based bioinks revealed the capacity of regulating cell behavior without influencing their printability and structural integrity following one week in cell culture.

A novel strategy that uses cell-laden core with a stable shell has been developed to create vascular-like structures. Cells encapsulated in the core/shell filaments showed increased cell viability during cultivation [67]. This strategy allows tuning the biophysical and biological properties of the vessel construct, and it has the advantage of fabricating multi-material and cellular constructs. To create blood vessel–like channels for nutrient and oxygen delivery within thick tissue constructs, a coaxial nozzle assembled bioprinting technique was developed by Zhang *et al.* by fabricating vessel-like printable microfluidic channels [70]. In this study, a pneumatic extrusion-assisted bioprinter using a coaxial needle was utilized to

Author Manuscript Author Manuscript Author Manuscript Author Manuscript

eject hollow alginate hydrogl strands containing cartilage progenitor cells. They evaluated two different sized coaxial nozzle assemblies: an assembly consist of 23-gauge inner needle (with 650 μm outer diameter (O.D.) and 330 μm inner diameter (I.D.)) and an 18-gauge outer needle (with 1270 μm O.D. and 840 μm I.D.). Another assembly consists of 26-gauge inner needle (with 457 μm O.D. and 230 μm I.D.) and an 18-gauge outer needle. The size of the inner nozzle was used to control the strand thickness, and thus the practical wall thickness. Similarly, Yu and co-workers developed a triaxial nozzle assembly to fabricate biocompatible cartilage-like tissues containing tubular channels encapsulated in alginate hydrogel [71]. They assessed two printing process factors inlcuding the size of coaxial assembly and alginate hydrogel dispensing pressures (i.e., 5 psi, 10 psi, and 20 psi).

In a similar fashion, Gao *et al.* printed high-strength sodium alginate hydrogels with built-in microchannels while controlling the crosslinking time to impose a higher resolution [72]. Later, Jia *et al.* created perusable vascular constructs via a multi-layered coaxial nozzle with concentric needles in one-step bioprinting, by mixing sodium alginate with poly(ethylene-glycol)-tetraacrylate (PEGTA) and GelMA pre-polymer solutions. In this blend bioink, the ionic crosslinking of alginate hydrogel was made by calcium ions and followed by photocrosslinking of GelMA and PEGTA used to tune the mechanical properties of printed constructs (Fig. 4D) [73]. Using the concept of embedded bioprinting, Christensen *et al.* fabricated vascular-like bifurcations with mouse fibroblast–laden alginate as the bioink and calcium chloride solution as the crosslinking agent [74]. Ionically crosslinkable alginate hydrogel by calcium chloride enables to develop the freeform inkjet printing technique by rapid solidifying of bioink and suspension features by providing a buoyant force. Similarly, an alginate-based hydrogel was embedded within gelatin bath for bioprinting of a trabeculated embryonic heart. Trabeculated embryonic hearts were printed using models from computed tomography and 3D optical images (Fig. 4E) [40].

3.2 Scaffold-free bioprinting

There are several limitations related to polymer and exogenous matrix-based tissues in development of 3D tissue constructs, such as unfavorable host response to biomaterials *in vivo* and necrosis by the limitation of nutrient diffusion [76–78]. Macroscopic scaffold-free technologies addressed these limitations by a combination of scaffold-free 3D cell culturing by using template and bioprinting. The novel fabrication methods to produce scaffold-free engineered tissue constructs have recently been developed [79, 80]. Scaffold-free methods can be associated with the low-adherence substrates which eliminate the creation of 2D monolayers. For instance, non-adherent plates can be utilized to promote attachment of cells to each other, or hanging drop methods can be used to eliminate cell-substrate interfaces and enable the production of 3D structure. One example is the use of non-adherent substrates and hepatic-destined cells to create vascularized liver tissue [77]. The migration of cells can be stimulated by the non-adherent surface where they self-organized into immature structures similar to liver.

The role of human tissue engineered myocardium in cardiac healing has been affected by several factors such as necrosis at the tissue core, immune response of scaffold materials, and deprived survival following ischemic or other damages associated by the transplantation

Author Manuscript Author Manuscript Author Manuscript Author Manuscript

of engineered tissue construct. Human cardiac muscle was fabricated by scaffold-free pre-vascularized cardiac tissue, which showed good *in vivo* transplantation and participation with the host coronary circulation [76]. Similar strategy was employed to make a scaffold-free vascular tissue [81]. Several vascular cell types comprising fibroblasts and smooth muscle cells were accumulated into distinct components, either multicellular spheroids or tubes of well-regulated diameters, ranging from 300 μm to 500 μm. They were printed with agarose rods as a non-adherent mold. The post-printing combination of the distinct components resulted in single- and double-layered vascular tubes (O.D. ranging 0.9–2.5 mm) [79–81]. Similarly, multiple cell types such as MSCs, fibroblast and endothelial cells, micro-patterned onto hydrogel through a layer-by layer bioprinting, were activated with maturation factors resulting in a vasculature formation which was confirmed by endothelial-specific gene expression [82]. A single feature of scaffold-free bioprinting techniques is the aptitude to engineer vessels of diverse forms and classified trees that combine tubes of discrete diameters. The method is rapid and precise, trustworthy and simply scalable. This study defines a method to form scaffold-free vascular constructs of distinct cellular organization and avoids the inadequacies related with scaffolds (Fig. 5) [81].

3.3 Free-standing bioprinting

Light-assisted bioprinting technologies allow fabricating core/shell structures with high aspect ratios by means of photolithography. Acellular vascular graft with inner diameters of 1 mm and wall thicknesses of 150 μm was fabricated by DMD-based stereolithography of poly(propylene fumarate) and tested *in vivo* [84]. The implants sustained patency and functionality up to six months in the venous system of mice. In addition, Two photon photolithography (TPP) along with polymer–protein hybrid materials have been used to fabricate small sized tubular constructs in the range of 10–100 μm [83, 85]. Given by the nonlinear nature of two-photon absorption, the polymerization only occurs around the focal point, which creates constructs with capillary-scale vasculature [86]. However, it suffers from very long fabrication processes that prevent scaling up and laser associated photo-bleaching [85]. Engelhardt *et al.* described facilitated function of TPP for biomaterial production [85]. They demonstrated the tissue engineering capabilities of TPP evidently enforced porcine chondrocytes to adjust their cell morphology by producing cross-linked gelatin microstructures. Polymer-protein hybrid microstructures were made where mainly the polymer functions as a backbone for the protein. For instance, diverse strain systems with protein membranes were produced. The TPP technique is the only freeform fabrication technique that acts in the complete composition range, thus can be used to artificially rebuild organ nanostructures and microstructures. Also, Ovsianikov *et al.* used a TPP fabricated gelatin scaffolds with 50 μm pillars and 250 μm × 250 μm pores loaded by MSCs [87].

4. Four-Dimensional (4D) Bioprinting

4.1 Biomaterials in 4D bioprinting

The dynamic environment of hydrogel scaffolds can be designed with chemical or physical functionalities to control time dimension. 4D bioprinting has been introduced in tissue engineering due to its intrinsic features such as (i) biofabrication of 3D scaffolds with programmable architectures using stimuli-responsive materials capable of changing their

Author Manuscript Author Manuscript Author Manuscript Author Manuscript

shape and function in response to external stimuli, and (ii) post-maturation of printed cells within scaffolds, generating complex tissue constructs with functions similar to native tissues. The fourth dimension, time, allows better mimicking the intrinsic dynamics and conformational changes of engineered tissues [88, 89]. The physical shape or function of 3D printed structure changes over time when an external stimulus such as *p*H [90], temperature [91], light [92], moisture [93], electric impulse [94] or magnetic field [95] is applied. 4D printed constructs are developed by two mechanisms. The first step is 3D bioprinting of stimuli-responsive materials, known as smart materials, that are capable of altering their chemical and/or physical properties in response to an external stimulus [89]. The second step is maturation of microengineered-tissue constructs after bioprinting through self-organization of cells, and/or matrix deposition forming functional tissue constructs gradually within a certain period [96]. Up to date, hydrogels [97] and shape memory polymers (SMPs) [98] are good candidates used in 4D bioprinting. Some of the commonly used stimuli to deform printed scaffolds are discussed here. We addressed some different stimuli-responsive 4D bioprinting techniques in Table 2.

4.1.1 Stimuli-responsive shape morphing

Moisture-responsive shape morphing: Due to water-saturated (swelling) nature of hydrogels, moisture is the most commonly used stimulus to deform a particular shape of printed scaffolds, where these scaffolds swell in a temporally and spatially coordinated manner when submerged in water. The moisture-induced deformation is dependent on the extent of water absorption (or swelling ratios) by printed scaffolds. A recently published 4D biomimetic printing technique used hydrogel composite bioink comprising an aqueous solution of N,N-dimethylacrylamide (or N-isopropylacrylamide for thermo-reversible systems), photoinitiator, nanoclay particles, glucose oxidase, glucose, and nanofibrillated cellulose to fabricate shape-morphing constructs analogous to natural flowers, bracts and leaves, transforming under stimulus, i.e. induced complex shape changes when immersed in water (Fig. 6A) [93]. Similarly, cell-laden bilayered photo-patterned PEG hydrogel constructs self-fold into cylindrical structures of different radii when immersed in aqueous solutions, with no adverse effect on the encapsulated cells (Fig. 6B) [99].

Temperature-responsive shape morphing: Temperature is another common stimulus used to deform thermosensitive materials, where some polymers have fluid-gel transition temperatures close to physiological temperature. These thermoresponsive polymers are widely used in various biomedical applications including drug delivery, gene delivery as well as in tissue engineering. For example, thermoresponsive 3D platform comprising poly(N-isopropylacrylamide) (PNIPAM) and ceramic powder (Al_2O_3) undergoes a fluid-gel transition in response to a thermal stimulus due to the phase transition of the graft chains (PNIPAM) [91].

Magnetic field-responsive shape morphing: Magnetic-responsive materials have gained significant interest due to their potential applications in biomedical, microfluidics and microelectronics fields. The magnetic field responsive materials are mainly comprised of a polymer matrix with embedded iron oxide nanoparticles. Similarly, polyurethane acrylate doped with alumina platelets, has been used to fabricate 4D scaffolds under low magnetic

Author Manuscript Author Manuscript Author Manuscript Author Manuscript

fields [95]. The orientation of printed anisotropic particles was controlled by applying magnetic field on printed constructs containing magnetized stiff platelets (for multi-material dispensers see Fig. 6C).

Light-responsive shape morphing: Light-responsive polymeric biomaterials are usually developed either by chemical incorporation of light-responsive chemical moieties into the polymer network or through mixed composite systems. Recently, DeForest *et al.* exploited three biorthogonal chemistries to obtain reversible and orientated immobilization of bioactive proteins with spatially and temporally controlled manner within cell-laden biomimetic scaffolds. To study the potential utility of the reversible, spatially controlled photomediated presentation of protein ligands, osteogenic differentiation of human MSCs was observed on the PEG-based polymeric network using photo-reversible patterning of vitronectin [92].

4.1.2 4D Bioprinting of vascularized tissue models—

4D bioprinting represents a promising approach to addressing the challenges related to the vascularization of engineered functional tissues, such as hollow tubular structures with high resolutions and biomimetic capillaries. Such approach allows the fabrication of hollow self- folding tubes with the control over the diameters and architectures of the generated tubes post-fabrication. Very recently, the versatility of the 4D bioprinting has been demonstrated by the fabrication of hollow self-folding tubes, with the control over diameters of the generated tubes at high resolution, using methacrylated alginate and hyaluronic acid hydrogels, and mouse bone marrow stromal cells [101]. This approach allowed the fabrication of hollow self-folding tubes with average internal diameters as small as 20 μm, which is comparable to the diameters of the smallest blood vessels (Fig. 6C). These self-folded hydrogel-based tubes support the survival of printed cells for at least 7 days without any negative effect on the viability of the cells [101]. In this direction, self-folding biocompatible polymers can be used in the fabrication of single or multilayered tube-like vessels by encapsulating different vascular cell types in the presence of external stimuli [81]. One example is recent advances in scaffold-free bioprinting of various vascular cell types, such as fibroblasts and smooth muscle cells, followed by their (environmental- and) time-dependent fusion into vascular tubes. Norotte *et al.* [81] described a self-assembly approach to engineer linear and branched vascular constructs of defined cellular composition and geometry using multicellular 3D spheroids or cylinders as building blocks. Various vascular cell types such as smooth muscle cells and fibroblasts, were aggregated into discrete units, either multicellular spheroids or cylinders of controllable diameter (300–500 μm). The multicellular spheroids were then deposited layer-by-layer with agarose rods which, upon cell fusion and maturation for 5–7 days, resulted in the final single- or double-layered vascular tubes [81] (Fig. 6D). 4D bioprinting of vascularized models is still in its infancy, and several challenges, such as spatiotemporal control of the stimuli responsive deformation of printed construct and localized control of cell orientation in vasculatures, need to be addressed.

4D bioprinting allows the precise control of the spatiotemporal distribution of different stimuli-responsive components that can fold/unfold to encapsulate and then release various therapeutic agents such as nano-drugs, growth factors or cells in a programmable manner.

Author Manuscript Author Manuscript Author Manuscript Author Manuscript

Bayley and colleagues fabricated tens of thousands of pico-liter aqueous droplets into a droplet of oil suspended in bulk aqueous solution [102]. The resulting oil droplets, known as multisomes, are cohesive and self-supporting which consist of aqueous micro-compartments bound together by lipid bilayers. Multisome network could be programmed by osmolarity gradients, which allow the network to fold/unfold into different complex structures. This method holds great potential for applications in controlled drug delivery. These self-folding printed multisome networks can be programmed to respond to changes in temperature, *p*H or chemical groups of the surrounding environment, enabling encapsulation and release of desirable therapeutic agents such as nano-drugs, macromolecular drugs or growth factors. Furthermore, these external stimuli-responsive droplets can further be integrated with microfluidics for capture, isolation and release of rare cells for diagnostic purposes.

4.1.3 Other applications of 4D Bioprinting—4D bioprinting concepts can be employed into drug loaded stents for vascular-targeted therapeutic approaches. Such system can be used to prevent the growth of plaques on stent implants in restenosis of arteries after angioplasty [103]. In a new trend, bioresorbable vascular stents have been developed, which are shown to be safe and efficacious alternatives to conventional metallic stents. The flexible tubular grids when deployed into the stenotic regions, they relieve an obstruction for the blood flow by pushing the vascular wall outwards [104]. 3D printed vascular stents have been developed using biodegradable, citric-acid-based polymer via contactless direct printing or stereo-lithography. Stents were prepared with a liquid photo-curable resin that is capable of printing objects with light. In addition, drugs were added to the citric-acid-based polymer that was released slowly at the site of the stent implantation that further improved the healing of the damaged blood vessel wall [105].

4D printing concepts have been exploited for fabricating protean medical devices such as splints that can be used for treating life-threatening diseases such as pediatric trachea-broncho-malacia (TBM). Using laser sintering, 3D printed airway splint was fabricated from polycaprolactone (PCL), which persists for two to three years before resorption *in vivo* [106]. This personalized bioresorbable medical device was designed to assist the growth of airway while preventing external compression over a designated period before bioresorption. The C-shaped tubular splints were successfully implanted around the collapsed airways and demonstrated that the shape and material of splints changed over time according to the patients' geometries and expanded with airway growth [107]. Splinted airways demonstrate improved patency and similar growth to normal airways.

4.2 Bioprinting towards drug delivery

4.2.1 Drug encapsulation in vascular implants—Hydrogel implants have been subjected to extensive research due to their promising applications in tissue engineering and carrier designs for drug delivery [108]. For carrier designs, and in particular for patterning proangiogenic factors and therapeutic molecules, the fabrication resolution is crucial to create the microenvironment in which drugs can be released with proper temporal and spatial distributions [109]. Recent studies on TPP has improved the resolution of 3D printing fabrication to a range lower than 100 nm [109]. 3D hydrogels fabricated by TPP are confronted with lower printing resolution imposed by scattering effects of the embedding

Author Manuscript Author Manuscript Author Manuscript Author Manuscript

fluid. Another issue is timing, which originates from the characteristics of two photon absorption and the absence of any water soluble and efficient initiators. Hence the spatial resolution depends on the laser scanning rate and the excitation power of the system [110]. These technical challenges would demand further research on TPP for fabricating drug-loaded vascular implants. Among the bioprinting strategies reviewed here, the core/shell design has great potentials for the creation of vascular delivery systems [111, 112]. The bottom-up nature of bioprinting approaches that form shell constructs through either direct-deposition or selective dissolution of the sacrificial core allows the encapsulation of cells during the fabrication process, such as alginate tubes scaffolds. Desired therapeutic molecules or proangiogenic factors can be easily partitioned within the core/shell structure, while the loading capacity, composition tunability and secreting actions of the design are the beneficial aspects of such core/shell systems. Drug-loaded core/shell implants provide safe loading of therapeutics in large quantities and multiple drug loading in a sustained manner [111]. In sacrificial bioprinting of core/shell constructs, the endothelial cells and growth factors can be loaded into the temporary core material to simultaneously make endothelial lining and promote capillary formation in the tubular construct. In summary, fine controls over the printing parameters make the core/shell design ideal for drug delivery systems and cell carriers, in particular when direct contact with blood circulation is required. The present knowledge on modifying bioink properties can be implemented into fine tuning of the shell layer (or layers) in order to regulate the fate of endothelial cells seeded within the channel.

4.2.2 Drug loaded stents—Advancements in bioresorbable stents along with current bioprinting techniques have opened a new avenue for potential drug delivery to placement site [113]. The stents are small, expandable tubular grids that are deployed into the stenotic regions in order to relieve an obstruction for the blood flow [104]. These bioresorbable polymer-based vascular stents are playing an important role in the treatment of vascular diseases such as coronary artery disease, peripheral arterial stenosis and aneurysms, and are shown to be safe and efficacious alternatives to conventional metallic stents. Based on physical–chemical characteristics of the vasculature, the endothelium can act as a barrier and as a potential target for drug delivery. The drug carriers can be conjugated with affinity moieties to bind endothelial cells for targeting pathologically altered endothelial cells. Recently printed vascular stents have been developed using biodegradable, citric-acid-based polymer via projection micro-stereo-lithography, as mentioned above. Other polymers used to manufacture bioabsorbable drug-eluting stents are mostly composed of polylactides such as polylactic acid or polycarbonate. 3D-printed poly (L-lactide)-based biodegradable stents were fabricated to deliver sirolimus loaded poly (D,L-lactide) nanoparticles. Sirolimus is an antiproliferative agent that has been used to prevent restenosis in coronary arteries. This drug-loaded nanoparticle coated drug-eluting stent showed pronounced inhibition effect on smooth muscle cell proliferation than on endothelial cell proliferation. A research group [114] used extrusion-assisted bioprinting to fabricate a bioresorbable, polycaprolactone-based stent coated with poly-(lactide-co-glycolide) and sirolimus. Although the geometry was strictly conformal to the cylindrical base used and limits the design freedom, it allows making drug loaded stents. Projection stereolithography was then used to perform fast printing by a dynamic digital mask [115]. Advances in 4D printing represent a major step toward the fabrication of personalized stents, but their delivery will likely require the

Author Manuscript Author Manuscript Author Manuscript Author Manuscript

development of new technologies to meet clinical expectations and improve patient outcome [116]. Patient-specific imaging and computational tools could be used to help the design and development of improved stent delivery catheters. Stimuli-responsive bioinks can be used to control the geometry and stiffness of the stent based on the pathological conditions of endothelial cells. Novel stimuli-responsive shape memory materials could be designed for fabricating drug-loaded stents.

4.2.3 Wound healing patches—Chronic wounds do not heal in an orderly fashion in part due to the lack of timely release of biological factors, oxygen and nutrients essential for healing. Developing a wound dressing that can deliver biomolecules and, at the same time, induce tissue regeneration would be beneficial for effective treatment of chronic wounds. In a recent study, a textile patch made of functional threads was developed for the treatment of chronic wounds [117] (Fig. 7D). The authors have fabricated an active wound dressing using composite fibers with a core electrical heater covered by a layer of polyethylene (glycol) diacrylate (PEGDA)-alginate hydrogel containing thermo-responsive drug carriers. Integrating the wound dressing with a prevascularized or angiogenic patch may address current challenges in chronic wound healing [118]. While the slow growth rate of blood vessels in angiogenic patches make them inappropriate for rapid vascularization of implants, prevascularized wound patches (tissue scaffolds seeded by vessel-forming cells) significantly improve the level of vascularization. Bioprinting techniques could provide various layers constructed modular or layer-by-layer with various cell types to promote the formation of the vascular networks for the complete regeneration of functional skin [119]. Modified inkjet printers are commonly used for ejecting nanoliter sized droplets of biological bioinks, including fibroblast, keratinocytes, melanocytes and sometimes stem cells to the construct [120]. Novel materials have also been introduced for fabricating wound dressing, such as nanocellulose made by a combination of carboxymethylation and periodate oxidation [121]. The outlook includes printed hydrogels that promote wound healing by either acting as a substrate for endogenous cell migration and proliferation or delivery carrier of potent cells. Nowadays dressings are designed for an optimum environment that includes a moist environment around the wound, effective oxygen circulation to aid regenerating cells and tissues and a low bacterial load.

4.2.4 Cardiac patches—Printed pre-vascularized cardiac patches have improved the therapeutic efficacy of cardiac repair by rapid vascularization post-transplantation. In one study, stem cells mixed with decellularized extracellular matrix and growth factors were used as a bioink system for extrusion bioprinting of layered (up to ten layers) cardiac patch [124]. They showed enhanced cardiac functions, reduced cardiac hypertrophy and fibrosis, as well as strong vascularization and tissue formation [124]. Using a different approach, scaffold-free printed cardiac patches were fabricated by growing human induced pluripotent stem cell-derived cardiomyocytes, fibroblasts and endothelial cells [125]. Immunostaining analyses of cardiomyocyte, fibroblast and endothelial cell markers revealed the rudimentary CD31+ blood vessel formation and the presence of the main cardiac gap junction protein, Connexin-43. Pre-vascularized cardiac patches, when loaded by cardio-responsive therapeutics, form the next generation of heart-related implants. Employment of bioprinting

Author Manuscript Author Manuscript Author Manuscript Author Manuscript

techniques can create new capacities in designing vasculature and patterning proangiogenic factors.

4.3 Drug screening chips

3D bioprinting has great potential to advance drug discovery and development, where it can be valuable for the study of molecular mechanisms of action, prioritization of drug candidates, toxicity testing and biomarker identification [126]. In such case, printed construct should have minimal functional units that recapitulate organ-level functions. Pathophysiological characteristics of diseased tissue microenvironment present multiple levels of transport barriers to targeted delivery of drugs [123] (Fig. 7B). To mechanistically understand the effects of microstructure on drug transport, printed chips that provide systematic control of relevant parameters and high content analysis of multifaceted drug transport are essential. All microstructure parameters are dynamic, interconnected, and may adversely affect the extravasation and interstitial transport of drugs. For example, in case of tumor microstructure the lack of interstitial fluid dynamics that is highly relevant to drug transport is one of the major limitations. Recent efforts to bioprint lab-on-chip models provide a robust and convenient platform to develop new targeted delivery strategies [127]. Advances in bioprinting together with novel bioinks now enable us with precise architectural control to fabricate biomimetic lab-on-chips that may better reproduce their vasculature and functions, and therefore provide accurate mechanistic studies as well as a tool for personalized therapeutics studies. Thus, engineered models of blood vessel and vasculature help the development of various vascular disease models, towards new therapeutics for atherosclerosis, hypertension, and many other disease conditions [9]. The reader is referred to existing reviews on vascular lab-on-chip models, for example, see Refs. [128, 129].

5. Concluding Remark and Future Directions

The classical strategy to create multiscale capillaries is to fabricate a large endothelialized vascular channel within the construct and tune the surrounding microstructure to induce capillary formation from the channel. These models lack directionality of vessel formation and cannot resemble the native vessels. We have reviewed current bioprinting techniques for fabricating vascularized models (see also Table 1). The use of sacrificial strategy with extrusion bioprinting has been employed by many researchers to fabricate vascular networks ranging in size from 100 μm to 1 mm. Extrusion-assisted bioprinting has been popular due to cost effectiveness, ease of control and the availability of shear-thinning bioinks. In addition, alginate-based bioinks have led to core/shell bioprinting of composite vascular systems. Light-assisted bioprinting when used with sacrificial or free-standing strategies offers a higher level of fabrication speed, better resolution and improved biocompatibility [127]. In particular, the use of DMD-based bioprinting systems has achieved the highest bioprinting speed. The experience gained on the therapeutic efficacy of 4D bioprinting techniques when used for tubular constructs presents novel solutions for vascular grafts and drug-loaded stents. However, there is a need to make precise multicellular structures with interconnected vascular network. A printed functional vasculature would support cells with oxygen exchange, nutrients, growth factors, and waste-product removal. The design of vasculature depends on not only the desired tissue but also the type of encapsulated cells

Author Manuscript Author Manuscript Author Manuscript Author Manuscript

within the printed construct. A simulation of how nutrition transport and amount of oxygen affect cells viability (e.g. the distance of nutrients diffusion) may help a better design of vasculature.

Bioprinting has shown a great promise in the current trend of personalized medicine, by customizing nutritional products, organs, and drugs [130] (Fig. 7). The technology advances are expected to fabricate complex heterogeneous tissues *in vitro*, such as liver and brain [131]. In addition, *in situ* printing of implants or living organs during operations was already performed for repairing external organs, such as skin [132]. In both cases, the vascular architecture should be tissue specific at microscale to meet the physiological functions and metabolic requirement for each tissue type [11]. On the other hand, the vascular geometry should minimize flow resistance within the construct at macroscale. A combination of bioprinting techniques and clinical imaging can lead to develop personalized tissue constructs. This will require a low-cost scale-up of customized vascular constructs that compromise between individuality and standardization [133]. The scale-up process not only depends on the fabrication process but also on imaging and computational modeling that allow monitoring cellular environment within the printed tissue. Development of imaging techniques greatly impacts the application of vascularized tissue constructs for tissue regeneration.

There are still two challenges to be addressed for making vascular tissue constructs. The first challenge is replicating the structural complexity and biological functionality of *in-vivo* vasculature, and the second challenge is how to integrate the vascular construct into a living host. The physical and structural properties of the vascularized construct must match those of native tissue. The desired physical properties could be achieved by optimizing bioink composition and introducing multi-material bioprinting techniques. Beyond the engineering of non-thrombogenic vessel constructs, controlling biological responses upon implantation should be considered. 4D bioprinting techniques allow fabricating vascular models that undergo site-specific remodeling. While we aim to scale up to whole organs, the biomolecular pathways that control organ specific heterogeneity of endothelial and vascular cells can be implemented into 4D bioprinting design. The future direction of this field is intended towards designing novel bioinks which change in physical properties over time.

Acknowledgements

The authors acknowledge funding from the National Institutes of Health (EB021857, AR066193, AR057837, CA214411, HL137193, EB024403, EB023052, EB022403), and Air Force Office of Sponsored Research under award # FA9550-15-1-0273. A.K.M. acknowledges the fellowships from the Fonds de Recherche du Québec–Santé (FRQS) and Canadian Institutes of Health Research (CIHR). S.M. acknowledges the American Fund for Alternatives to Animal Research for AFAAR Postdoctoral Fellowship. S.R.S. would like to thank Brigham and Women's Hospital President Betsy Nabel, MD, and the Reny family, for the Stepping Strong Innovator Award.

References

[1]. Laschke MW, Harder Y, Amon M, Martin I, Farhadi J, Ring A, et al. Angiogenesis in tissue engineering: breathing life into constructed tissue substitutes. Tissue engineering. 2006;12:2093–104. [PubMed: 16968151]

[2]. Bae H, Puranik AS, Gauvin R, Edalat F, Carrillo-Conde B, Peppas NA, et al. Building vascular networks. Science translational medicine. 2012;4:160ps23–ps23.

Author Manuscript Author Manuscript Author Manuscript Author Manuscript

[3]. Fukuda S, Yoshii S, Kaga S, Matsumoto M, Kugiyama K, Maulik N. Angiogenic strategy for human ischemic heart disease: brief overview. Molecular and cellular biochemistry. 2004;264:143–9. [PubMed: 15544043]

[4]. Bennett S, Griffiths G, Schor A, Leese G, Schor S. Growth factors in the treatment of diabetic foot ulcers. British Journal of Surgery. 2003;90:133–46. [PubMed: 12555288]

[5]. Kaully T, Kaufman-Francis K, Lesman A, Levenberg S. Vascularization—the conduit to viable engineered tissues. Tissue Engineering Part B: Reviews. 2009;15:159–69. [PubMed: 19309238]

[6]. Kolesky DB, Homan KA, Skylar-Scott MA, Lewis JA. Three-dimensional bioprinting of thick vascularized tissues. Proceedings of the National Academy of Sciences. 2016;113:3179–84.

[7]. Atala A, Kasper FK, Mikos AG. Engineering complex tissues. Science translational medicine. 2012;4:160rv12–rv12.

[8]. Guillemette MD, Gauvin R, Perron C, Labbe R, Germain L, Auger FA. Tissue-engineered vascular adventitia with vasa vasorum improves graft integration and vascularization through inosculation. Tissue Engineering Part A. 2010;16:2617–26. [PubMed: 20455774]

[9]. Richards D, Jia J, Yost M, Markwald R, Mei Y. 3D bioprinting for vascularized tissue fabrication. Annals of biomedical engineering. 2017;45:132–47. [PubMed: 27230253]

[10]. Bao P, Kodra A, Tomic-Canic M, Golinko MS, Ehrlich HP, Brem H. The role of vascular endothelial growth factor in wound healing. Journal of Surgical Research. 2009;153:347–58. [PubMed: 19027922]

[11]. Paulsen SJ, Miller JS. Tissue vascularization through 3D printing: Will technology bring us flow? Developmental Dynamics. 2015;244:629–40. [PubMed: 25613150]

[12]. Ehrbar M, Djonov VG, Schnell C, Tschanz SA, Martiny-Baron G, Schenk U, et al. Cell-demanded liberation of VEGF121 from fibrin implants induces local and controlled blood vessel growth. Circulation research. 2004;94:1124–32. [PubMed: 15044320]

[13]. Martineau L, Doillon CJ. Angiogenic response of endothelial cells seeded dispersed versus on beads in fibrin gels. Angiogenesis. 2007;10:269–77. [PubMed: 17721825]

[14]. Borenstein JT, Terai H, King KR, Weinberg E, Kaazempur-Mofrad M, Vacanti J. Microfabrication technology for vascularized tissue engineering. Biomedical microdevices. 2002;4:167–75.

[15]. Klar AS, Güven S, Biedermann T, Luginbühl J, Böttcher-Haberzeth S, Meuli-Simmen C, et al. Tissue-engineered dermo-epidermal skin grafts prevascularized with adipose-derived cells. Biomaterials. 2014;35:5065–78. [PubMed: 24680190]

[16]. Zhu W, Qu X, Zhu J, Ma X, Patel S, Liu J, et al. Direct 3D bioprinting of prevascularized tissue constructs with complex microarchitecture. Biomaterials. 2017;124:106–15. [PubMed: 28192772]

[17]. Koike N, Fukumura D, Gralla O, Au P, Schechner JS, Jain RK. Tissue engineering: creation of long-lasting blood vessels. Nature. 2004;428:138–9. [PubMed: 15014486]

[18]. Sorrell JM, Baber MA, Caplan AI. Influence of adult mesenchymal stem cells on in vitro vascular formation. Tissue Engineering Part A. 2009;15:1751–61. [PubMed: 19196139]

[19]. Ford MC, Bertram JP, Hynes SR, Michaud M, Li Q, Young M, et al. A macroporous hydrogel for the coculture of neural progenitor and endothelial cells to form functional vascular networks invivo. Proceedings of the National Academy of Sciences of the United States of America. 2006;103:2512–7. [PubMed: 16473951]

[20]. Liu J, Zheng H, Poh PS, Machens H-G, Schilling AF. Hydrogels for engineering of perfusable vascular networks. International journal of molecular sciences. 2015;16:15997–6016. [PubMed: 26184185]

[21]. Hasan A, Paul A, Memic A, Khademhosseini A. A multilayered microfluidic blood vessel-like structure. Biomedical microdevices. 2015;17:88. [PubMed: 26256481]

[22]. Ling Y, Rubin J, Deng Y, Huang C, Demirci U, Karp JM, et al. A cell-laden microfluidic hydrogel. Lab on a Chip. 2007;7:756–62. [PubMed: 17538718]

[23]. Francis ME, Uriel S, Brey EM. Endothelial cell–matrix interactions in neovascularization. Tissue Engineering Part B: Reviews. 2008;14:19–32. [PubMed: 18454632]

[24]. Clauss M, Breier G. Mechanisms of angiogenesis: Springer Science & Business Media; 2004.

Author Manuscript Author Manuscript Author Manuscript Author Manuscript

[25]. Song HHG, Rumma RT, Ozaki CK, Edelman ER, Chen CS. Vascular Tissue Engineering: Progress, Challenges, and Clinical Promise. Cell Stem Cell. 2018;22:340–54. [PubMed: 29499152]

[26]. Amensag S, McFetridge PS. Rolling the human amnion to engineer laminated vascular tissues. Tissue Engineering Part C: Methods. 2012;18:903–12. [PubMed: 22616610]

[27]. Tschoeke B, Flanagan TC, Cornelissen A, Koch S, Roehl A, Sriharwoko M, et al. Development of a Composite Degradable/Nondegradable Tissue-engineered Vascular Graft. Artificial organs. 2008;32:800–9. [PubMed: 18684200]

[28]. Guillotin B, Guillemot F. Cell patterning technologies for organotypic tissue fabrication. Trends in biotechnology. 2011;29:183–90. [PubMed: 21256609]

[29]. Cui X, Boland T, D D'Lima D, K Lotz M. Thermal inkjet printing in tissue engineering and regenerative medicine. Recent patents on drug delivery & formulation. 2012;6:149–55. [PubMed: 22436025]

[30]. Bhuthalingam R, Lim PQ, Irvine SA, Agrawal A, Mhaisalkar PS, An J, et al. A novel 3D printing method for cell alignment and differentiation. International Journal of Bioprinting. 2015;1.

[31]. Jia J, Richards DJ, Pollard S, Tan Y, Rodriguez J, Visconti RP, et al. Engineering alginate as bioink for bioprinting. Acta biomaterialia. 2014;10:4323–31. [PubMed: 24998183]

[32]. Khalil S, Sun W. Bioprinting endothelial cells with alginate for 3D tissue constructs. Journal of biomechanical engineering. 2009;131:111002. [PubMed: 20353253]

[33]. Bertassoni LE, Cardoso JC, Manoharan V, Cristino AL, Bhise NS, Araujo WA, et al. Direct-write Bioprinting of Cell-laden Methacrylated Gelatin Hydrogels. Biofabrication. 2014;6:024105-. [PubMed: 24695367]

[34]. Kolesky DB, Truby RL, Gladman A, Busbee TA, Homan KA, Lewis JA. 3D bioprinting of vascularized, heterogeneous cell-laden tissue constructs. Advanced materials. 2014;26:3124–30. [PubMed: 24550124]

[35]. Bertassoni LE, Cecconi M, Manoharan V, Nikkhah M, Hjortnaes J, Cristino AL, et al. Hydrogel bioprinted microchannel networks for vascularization of tissue engineering constructs. Lab on a Chip. 2014;14:2202–11. [PubMed: 24860845]

[36]. Liu W, Zhang YS, Heinrich MA, De Ferrari F, Jang HL, Bakht SM, et al. Rapid continuous multimaterial extrusion bioprinting. Advanced Materials. 2017;29.

[37]. Datta P, Ayan B, Ozbolat IT. Bioprinting for vascular and vascularized tissue biofabrication. Acta biomaterialia. 2017.

[38]. Jungst T, Smolan W, Schacht K, Scheibel T, Groll Jr. Strategies and molecular design criteria for 3D printable hydrogels. Chemical reviews. 2015;116:1496–539. [PubMed: 26492834]

[39]. Murphy SV, Atala A. 3D bioprinting of tissues and organs. Nature biotechnology. 2014;32:773–85.

[40]. Hinton TJ, Jallerat Q, Palchesko RN, Park JH, Grodzicki MS, Shue H-J, et al. Three-dimensional printing of complex biological structures by freeform reversible embedding of suspended hydrogels. Science advances. 2015;1:e1500758. [PubMed: 26601312]

[41]. Chang CC, Boland ED, Williams SK, Hoying JB. Direct-write bioprinting three-dimensional biohybrid systems for future regenerative therapies. Journal of Biomedical Materials Research Part B: Applied Biomaterials. 2011;98:160–70.

[42]. Mandrycky C, Wang Z, Kim K, Kim D-H. 3D bioprinting for engineering complex tissues. Biotechnology advances. 2016;34:422–34. [PubMed: 26724184]

[43]. Ruel-Gariepy E, Leroux J-C. In situ-forming hydrogels—review of temperature-sensitive systems. European Journal of Pharmaceutics and Biopharmaceutics. 2004;58:409–26. [PubMed: 15296964]

[44]. Zhang YS, Davoudi F, Walch P, Manbachi A, Luo X, Dell'Erba V, et al. Bioprinted thrombosis-on-a-chip. Lab on a Chip. 2016;16:4097–105. [PubMed: 27722710]

[45]. Lee VK, Lanzi AM, Ngo H, Yoo S-S, Vincent PA, Dai G. Generation of multi-scale vascular network system within 3D hydrogel using 3D bio-printing technology. Cellular and molecular bioengineering. 2014;7:460–72. [PubMed: 25484989]

[46]. Wu W, DeConinck A, Lewis JA. Omnidirectional printing of 3D microvascular networks. Advanced Materials. 2011;23.

Author Manuscript Author Manuscript Author Manuscript Author Manuscript

[47]. Homan KA, Kolesky DB, Skylar-Scott MA, Herrmann J, Obuobi H, Moisan A, et al. Bioprinting of 3D convoluted renal proximal tubules on perfusable chips. Scientific reports. 2016;6:34845. [PubMed: 27725720]

[48]. Lee VK, Kim DY, Ngo H, Lee Y, Seo L, Yoo S-S, et al. Creating perfused functional vascular channels using 3D bio-printing technology. Biomaterials. 2014;35:8092–102. [PubMed: 24965886]

[49]. Nguyen D-HT, Stapleton SC, Yang MT, Cha SS, Choi CK, Galie PA, et al. Biomimetic model to reconstitute angiogenic sprouting morphogenesis in vitro. Proceedings of the National Academy of Sciences. 2013;110:6712–7.

[50]. Miller JS, Stevens KR, Yang MT, Baker BM, Nguyen D-HT, Cohen DM, et al. Rapid casting of patterned vascular networks for perfusable engineered three-dimensional tissues. Nature materials. 2012;11:768–74. [PubMed: 22751181]

[51]. Sooppan R, Paulsen SJ, Han J, Ta AH, Dinh P, Gaffey AC, et al. In vivo anastomosis and perfusion of a three-dimensionally-printed construct containing microchannel networks. Tissue Engineering Part C: Methods. 2015;22:1–7. [PubMed: 26414863]

[52]. Boland T, Xu T, Damon B, Cui X. Application of inkjet printing to tissue engineering. Biotechnology journal. 2006;1:910–7. [PubMed: 16941443]

[53]. Saunders RE, Gough JE, Derby B. Delivery of human fibroblast cells by piezoelectric drop-on-demand inkjet printing. Biomaterials. 2008;29:193–203. [PubMed: 17936351]

[54]. Nishiyama Y, Henmi C, Iwanaga S, Nakagawa H, Yamaguchi K, Akita K, et al. Ink jet three-dimensional digital fabrication for biological tissue manufacturing: analysis of alginate microgel beads produced by ink jet droplets for three dimensional tissue fabrication. Journal of Imaging Science and Technology. 2008;52:60201–1−-6.

[55]. Nishiyama Y, Nakamura M, Henmi C, Yamaguchi K, Mochizuki S, Nakagawa H, et al. Development of a three-dimensional bioprinter: construction of cell supporting structures using hydrogel and state-of-the-art inkjet technology. Journal of Biomechanical Engineering. 2009;131:035001. [PubMed: 19154078]

[56]. Pataky K, Braschler T, Negro A, Renaud P, Lutolf MP, Brugger J. Microdrop Printing of Hydrogel Bioinks into 3D Tissue-Like Geometries. Advanced Materials. 2012;24:391–6. [PubMed: 22161949]

[57]. Cui X, Boland T. Human microvasculature fabrication using thermal inkjet printing technology. Biomaterials. 2009;30:6221–7. [PubMed: 19695697]

[58]. Huang TQ, Qu X, Liu J, Chen S. 3D printing of biomimetic microstructures for cancer cell migration. Biomedical microdevices. 2014;16:127–32. [PubMed: 24150602]

[59]. Xu T, Jin J, Gregory C, Hickman JJ, Boland T. Inkjet printing of viable mammalian cells. Biomaterials. 2005;26:93–9. [PubMed: 15193884]

[60]. Guillemot F, Souquet A, Catros S, Guillotin B, Lopez J, Faucon M, et al. High-throughput laser printing of cells and biomaterials for tissue engineering. Acta biomaterialia. 2010;6:2494–500. [PubMed: 19819356]

[61]. Wu P, Ringeisen B. Development of human umbilical vein endothelial cell (HUVEC) and human umbilical vein smooth muscle cell (HUVSMC) branch/stem structures on hydrogel layers via biological laser printing (BioLP). Biofabrication. 2010;2:014111. [PubMed: 20811126]

[62]. Barron J, Wu P, Ladouceur H, Ringeisen B. Biological laser printing: a novel technique for creating heterogeneous 3-dimensional cell patterns. Biomedical microdevices. 2004;6:139–47. [PubMed: 15320636]

[63]. Guillotin B, Souquet A, Catros S, Duocastella M, Pippenger B, Bellance S, et al. Laser assisted bioprinting of engineered tissue with high cell density and microscale organization. Biomaterials. 2010;31:7250–6. [PubMed: 20580082]

[64]. Cha C, Soman P, Zhu W, Nikkhah M, Camci-Unal G, Chen S, et al. Structural reinforcement of cell-laden hydrogels with microfabricated three dimensional scaffolds. Biomaterials science. 2014;2:703–9. [PubMed: 24778793]

[65]. Han L-H, Suri S, Schmidt CE, Chen S. Fabrication of three-dimensional scaffolds for heterogeneous tissue engineering. Biomedical microdevices. 2010;12:721–5. [PubMed: 20393801]

Author Manuscript Author Manuscript Author Manuscript Author Manuscript

[66]. Miri AK, Nieto D, Iglesias L, Goodarzi Hosseinabadi H, Maharjan S, Ruiz-Esparza GU, et al. Microfluidics-Enabled Multimaterial Maskless Stereolithographic Bioprinting. Advanced Materials. 2018:1800242.

[67]. Mistry P, Aied A, Alexander M, Shakesheff K, Bennett A, Yang J. Bioprinting Using Mechanically Robust Core–Shell Cell-Laden Hydrogel Strands. Macromolecular Bioscience. 2017.

[68]. Axpe E, Oyen ML. Applications of alginate-based bioinks in 3D bioprinting. International journal of molecular sciences. 2016;17:1976.

[69]. Lee KY, Mooney DJ. Alginate: properties and biomedical applications. Progress in polymer science. 2012;37:106–26. [PubMed: 22125349]

[70]. Zhang Y, Yu Y, Chen H, Ozbolat IT. Characterization of printable cellular micro-fluidic channels for tissue engineering. Biofabrication. 2013;5:025004. [PubMed: 23458889]

[71]. Yu Y, Zhang Y, Martin JA, Ozbolat IT. Evaluation of cell viability and functionality in vessel-like bioprintable cell-laden tubular channels. Journal of biomechanical engineering. 2013;135:091011.

[72]. Gao Q, He Y, Fu J-z, Liu A, Ma L. Coaxial nozzle-assisted 3D bioprinting with built-in microchannels for nutrients delivery. Biomaterials. 2015;61:203–15. [PubMed: 26004235]

[73]. Jia W, Gungor-Ozkerim PS, Zhang YS, Yue K, Zhu K, Liu W, et al. Direct 3D bioprinting of perfusable vascular constructs using a blend bioink. Biomaterials. 2016;106:58–68. [PubMed: 27552316]

[74]. Christensen K, Xu C, Chai W, Zhang Z, Fu J, Huang Y. Freeform inkjet printing of cellular structures with bifurcations. Biotechnology and bioengineering. 2015;112:1047–55. [PubMed: 25421556]

[75]. Akkineni AR, Ahlfeld T, Lode A, Gelinsky M. A versatile method for combining different biopolymers in a core/shell fashion by 3D plotting to achieve mechanically robust constructs. Biofabrication. 2016;8:045001. [PubMed: 27716641]

[76]. Stevens K, Kreutziger K, Dupras S, Korte F, Regnier M, Muskheli V, et al. Physiological function and transplantation of scaffold-free and vascularized human cardiac muscle tissue. Proceedings of the National Academy of Sciences. 2009;106:16568–73.

[77]. Takebe T, Sekine K, Enomura M, Koike H, Kimura M, Ogaeri T, et al. Vascularized and functional human liver from an iPSC-derived organ bud transplant. Nature. 2013;499:481–4. [PubMed: 23823721]

[78]. Tan Y, Richards DJ, Trusk TC, Visconti RP, Yost MJ, Kindy MS, et al. 3D printing facilitated scaffold-free tissue unit fabrication. Biofabrication. 2014;6:024111. [PubMed: 24717646]

[79]. Baptista PM, Vyas D, Moran E, Wang Z, Soker S. Human liver bioengineering using a whole liver decellularized bioscaffold. Organ Regeneration: Methods and Protocols. 2013:289–98.

[80]. Ruedinger F, Lavrentieva A, Blume C, Pepelanova I, Scheper T. Hydrogels for 3D mammalian cell culture: a starting guide for laboratory practice. Applied microbiology and biotechnology. 2015;99:623–36. [PubMed: 25432676]

[81]. Norotte C, Marga FS, Niklason LE, Forgacs G. Scaffold-free vascular tissue engineering using bioprinting. Biomaterials. 2009;30:5910–7. [PubMed: 19664819]

[82]. Hong S, Song S-J, Lee JY, Jang H, Choi J, Sun K, et al. Cellular behavior in micropatterned hydrogels by bioprinting system depended on the cell types and cellular interaction. Journal of bioscience and bioengineering. 2013;116:224–30. [PubMed: 23562089]

[83]. Meyer W, Engelhardt S, Novosel E, Elling B, Wegener M, Krüger H. Soft Polymers for Building up Small and Smallest Blood Supplying Systems by Stereolithography. Journal of Functional Biomaterials. 2012;3:257–68. [PubMed: 24955530]

[84]. Melchiorri AJ, Hibino N, Best C, Yi T, Lee Y, Kraynak C, et al. 3D-Printed Biodegradable Polymeric Vascular Grafts. Advanced healthcare materials. 2016;5:319–25. [PubMed: 26627057]

[85]. Engelhardt S, Hoch E, Borchers K, Meyer W, Krüger H, Tovar GE, et al. Fabrication of 2D protein microstructures and 3D polymer–protein hybrid microstructures by two-photon polymerization. Biofabrication. 2011;3:025003. [PubMed: 21562366]

Author Manuscript Author Manuscript Author Manuscript Author Manuscript

[86]. Sazer D, Miller J. Vascular Networks Within 3D Printed and Engineered Tissues In: Ovsianikov A, Yoo J, Mironov V, editors. 3D Printing and Biofabrication. Cham: Springer International Publishing; 2017 p. 1–27.

[87]. Ovsianikov A, Deiwick A, Van Vlierberghe S, Dubruel P, Möller L, Dräger G, et al. Laser fabrication of three-dimensional CAD scaffolds from photosensitive gelatin for applications in tissue engineering. Biomacromolecules. 2011;12:851–8. [PubMed: 21366287]

[88]. Gao B, Yang Q, Zhao X, Jin G, Ma Y, Xu F. 4D bioprinting for biomedical applications. Trends in biotechnology. 2016;34:746–56. [PubMed: 27056447]

[89]. Tibbits S 4D printing: multi-material shape change. Architectural Design. 2014;84:116–21.

[90]. Villar G, Heron AJ, Bayley H. Formation of droplet networks that function in aqueous environments. Nature nanotechnology. 2011;6:803–8.

[91]. Wang T, Zheng S, Sun W, Liu X, Fu S, Tong Z. Notch insensitive and self-healing PNIPAm–PAM–clay nanocomposite hydrogels. Soft Matter. 2014;10:3506–12. [PubMed: 24652073]

[92]. DeForest CA, Tirrell DA. A photoreversible protein-patterning approach for guiding stem cell fate in three-dimensional gels. Nature materials. 2015;14:523–31. [PubMed: 25707020]

[93]. Gladman AS, Matsumoto EA, Nuzzo RG, Mahadevan L, Lewis JA. Biomimetic 4D printing. Nature materials. 2016;15:413–8. [PubMed: 26808461]

[94]. Dvir T, Timko BP, Kohane DS, Langer R. Nanotechnological strategies for engineering complex tissues. Nature nanotechnology. 2011;6:13–22.

[95]. Kokkinis D, Schaffner M, Studart AR. Multimaterial magnetically assisted 3D printing of composite materials. Nature communications. 2015;6:8643.

[96]. Khoo ZX, Teoh JEM, Liu Y, Chua CK, Yang S, An J, et al. 3D printing of smart materials: A review on recent progresses in 4D printing. Virtual and Physical Prototyping. 2015;10:103–22.

[97]. Erb RM, Sander JS, Grisch R, Studart AR. Self-shaping composites with programmable bioinspired microstructures. Nature communications. 2013;4:1712.

[98]. Behl M, Razzaq MY, Lendlein A. Multifunctional Shape-Memory Polymers. Advanced materials. 2010;22:3388–410. [PubMed: 20574951]

[99]. Jamal M, Kadam SS, Xiao R, Jivan F, Onn TM, Fernandes R, et al. Bio-Origami Hydrogel Scaffolds Composed of Photocrosslinked PEG Bilayers. Advanced healthcare materials. 2013;2:1142–50. [PubMed: 23386382]

[100]. Bakarich SE, Gorkin R, Spinks GM. 4D printing with mechanically robust, thermally actuating hydrogels. Macromolecular rapid communications. 2015;36:1211–7. [PubMed: 25864515]

[101]. Kirillova A, Maxson R, Stoychev G, Gomillion CT, Ionov L. 4D Biofabrication Using Shape-Morphing Hydrogels. Advanced Materials. 2017;29.

[102]. Villar G, Graham AD, Bayley H. A Tissue-Like Printed Material. Science (New York, NY). 2013;340:48–52.

[103]. Koren E, Torchilin VP. Drug carriers for vascular drug delivery. IUBMB life. 2011;63:586–95. [PubMed: 21766415]

[104]. Flórez-Valencia L, Orkisz M, Montagnat J. 3D graphical models for vascular-stent pose simulation. Machine Graphics and vision. 2004;13:235–48.

[105]. van Lith R, Baker E, Ware H, Yang J, Farsheed AC, Sun C, et al. 3D-Printing Strong High-Resolution Antioxidant Bioresorbable Vascular Stents. Advanced Materials Technologies. 2016;1.

[106]. Kinstlinger IS, Bastian A, Paulsen SJ, Hwang DH, Ta AH, Yalacki DR, et al. Open-source selective laser sintering (OpenSLS) of nylon and biocompatible polycaprolactone. PloS one. 2016;11:e0147399. [PubMed: 26841023]

[107]. Morrison RJ, Hollister SJ, Niedner MF, Mahani MG, Park AH, Mehta DK, et al. Mitigation of tracheobronchomalacia with 3D-printed personalized medical devices in pediatric patients. Science translational medicine. 2015;7:285ra64–ra64.

[108]. Ciuciu AI, Cywiński PJ. Two-photon polymerization of hydrogels–versatile solutions to fabricate well-defined 3D structures. RSC Advances. 2014;4:45504–16.

Author Manuscript Author Manuscript Author Manuscript Author Manuscript

[109]. Raimondi MT, Eaton SM, Nava MM, Laganà M, Cerullo G, Osellame R. Two-photon laser polymerization: from fundamentals to biomedical application in tissue engineering and regenerative medicine. J Appl Biomater Biomech. 2012;10:55–65.

[110]. Xing J-F, Zheng M-L, Duan X-M. Two-photon polymerization microfabrication of hydrogels: an advanced 3D printing technology for tissue engineering and drug delivery. Chemical Society Reviews. 2015;44:5031–9. [PubMed: 25992492]

[111]. Perez RA, Kim H-W. Core–shell designed scaffolds for drug delivery and tissue engineering. Acta Biomaterialia. 2015;21:2–19. [PubMed: 25792279]

[112]. Moroni L, Schotel R, Sohier J, de Wijn JR, van Blitterswijk CA. Polymer hollow fiber three-dimensional matrices with controllable cavity and shell thickness. Biomaterials. 2006;27:5918–26. [PubMed: 16935328]

[113]. Acharya G, Park K. Mechanisms of controlled drug release from drug-eluting stents. Advanced Drug Delivery Reviews. 2006;58:387–401. [PubMed: 16546289]

[114]. Park SA, Lee SJ, Lim KS, Bae IH, Lee JH, Kim WD, et al. In vivo evaluation and characterization of a bio-absorbable drug-coated stent fabricated using a 3D-printing system. Materials Letters. 2015;141:355–8.

[115]. Gross BC, Erkal JL, Lockwood SY, Chen C, Spence DM. Evaluation of 3D printing and its potential impact on biotechnology and the chemical sciences. ACS Publications; 2014.

[116]. Ameer GA, Akar B, Sun C. 3D-printed bioresorbable vascular scaffolds: an important step towards personalizing vascular medical devices? : Taylor & Francis; 2017.

[117]. Mostafalu P, Kiaee G, Giatsidis G, Khalilpour A, Nabavinia M, Dokmeci MR, et al. A Textile Dressing for Temporal and Dosage Controlled Drug Delivery. Advanced Functional Materials. 2017.

[118]. Frueh FS, Menger MD, Lindenblatt N, Giovanoli P, Laschke MW. Current and emerging vascularization strategies in skin tissue engineering. Critical reviews in biotechnology. 2017;37:613–25. [PubMed: 27439727]

[119]. Velasquillo C, Galue EA, Rodriquez L, Ibarra C, Ibarra-Ibarra LG. Skin 3D bioprinting. Applications in cosmetology. Journal of Cosmetics, Dermatological Sciences and Applications. 2013;3:85.

[120]. He P, Zhao J, Zhang J, Li B, Gou Z, Gou M, et al. Bioprinting of skin constructs for wound healing. Burns & trauma. 2018;6:5. [PubMed: 29404374]

[121]. Rees A, Powell LC, Chinga-Carrasco G, Gethin DT, Syverud K, Hill KE, et al. 3D Bioprinting of Carboxymethylated-Periodate Oxidized Nanocellulose Constructs for Wound Dressing Applications. BioMed Research International. 2015;2015:925757. [PubMed: 26090461]

[122]. Zhu Y, Hu C, Li B, Yang H, Cheng Y, Cui W. A highly flexible paclitaxel-loaded poly (ε-caprolactone) electrospun fibrous-membrane-covered stent for benign cardia stricture. Acta biomaterialia. 2013;9:8328–36. [PubMed: 23770223]

[123]. Zheng Y, Chen J, Craven M, Choi NW, Totorica S, Diaz-Santana A, et al. In vitro microvessels for the study of angiogenesis and thrombosis. Proceedings of the National Academy of Sciences. 2012;109:9342–7.

[124]. Jang J, Park H-J, Kim S-W, Kim H, Park JY, Na SJ, et al. 3D printed complex tissue construct using stem cell-laden decellularized extracellular matrix bioinks for cardiac repair. Biomaterials. 2017;112:264–74. [PubMed: 27770630]

[125]. Ong CS, Fukunishi T, Zhang H, Huang CY, Nashed A, Blazeski A, et al. Biomaterial-Free Three-Dimensional Bioprinting of Cardiac Tissue using Human Induced Pluripotent Stem Cell Derived Cardiomyocytes. Scientific Reports. 2017;7.

[126]. Bhatia SN, Ingber DE. Microfluidic organs-on-chips. Nat Biotech. 2014;32:760–72.

[127]. Urrios A, Parra-Cabrera C, Bhattacharjee N, Gonzalez-Suarez AM, Rigat-Brugarolas LG, Nallapatti U, et al. 3D-printing of transparent bio-microfluidic devices in PEG-DA. Lab on a Chip. 2016;16:2287–94. [PubMed: 27217203]

[128]. Dittrich PS, Manz A. Lab-on-a-chip: microfluidics in drug discovery. Nature reviews Drug discovery. 2006;5:210. [PubMed: 16518374]

[129]. Khalid N, Kobayashi I, Nakajima M. Recent lab-on-chip developments for novel drug discovery. Wiley Interdisciplinary Reviews: Systems Biology and Medicine. 2017.

Author Manuscript Author Manuscript Author Manuscript Author Manuscript

[130]. Ventola CL. Medical applications for 3D printing: current and projected uses. Pharmacy and Therapeutics. 2014;39:704. [PubMed: 25336867]

[131]. Lipson H. New world of 3-D printing offers" completely new ways of thinking": Q&A with author, engineer, and 3-D printing expert Hod Lipson. IEEE pulse. 2012;4:12–4.

[132]. Binder KW, Zhao W, Aboushwareb T, Dice D, Atala A, Yoo JJ. In situ bioprinting of the skin for burns. Journal of the American College of Surgeons. 2010;211:S76.

[133]. Elomaa L, Yang YP. Additive manufacturing of vascular grafts and vascularized tissue constructs. Tissue Engineering Part B: Reviews. 2017.

Author Manuscript Author Manuscript Author Manuscript Author Manuscript

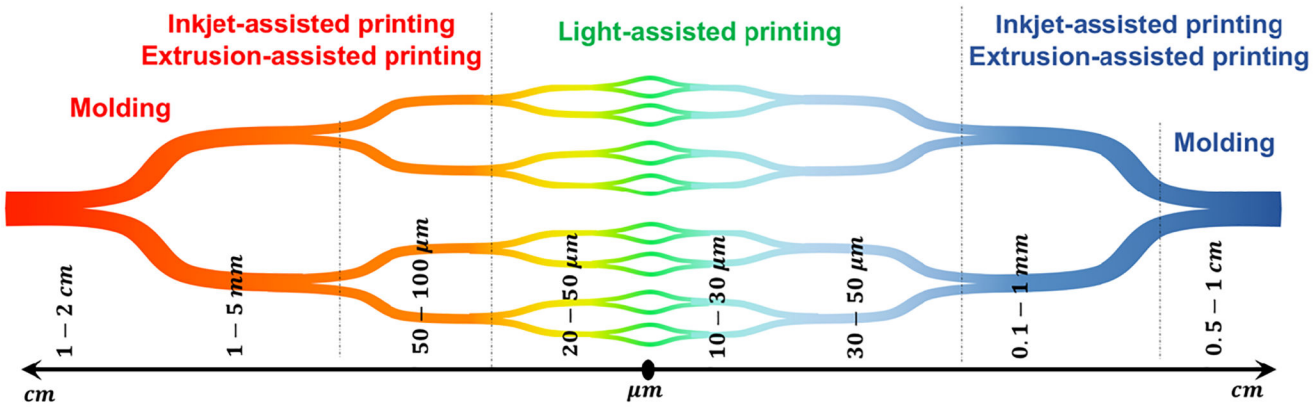

Fig. 1.

The summary of blood vessel hierarchy (from arteries to veins) in the body and the range of diameters at each level, along with current fabrication techniques used to engineer biomimetic tissue construct.

Author Manuscript Author Manuscript Author Manuscript Author Manuscript

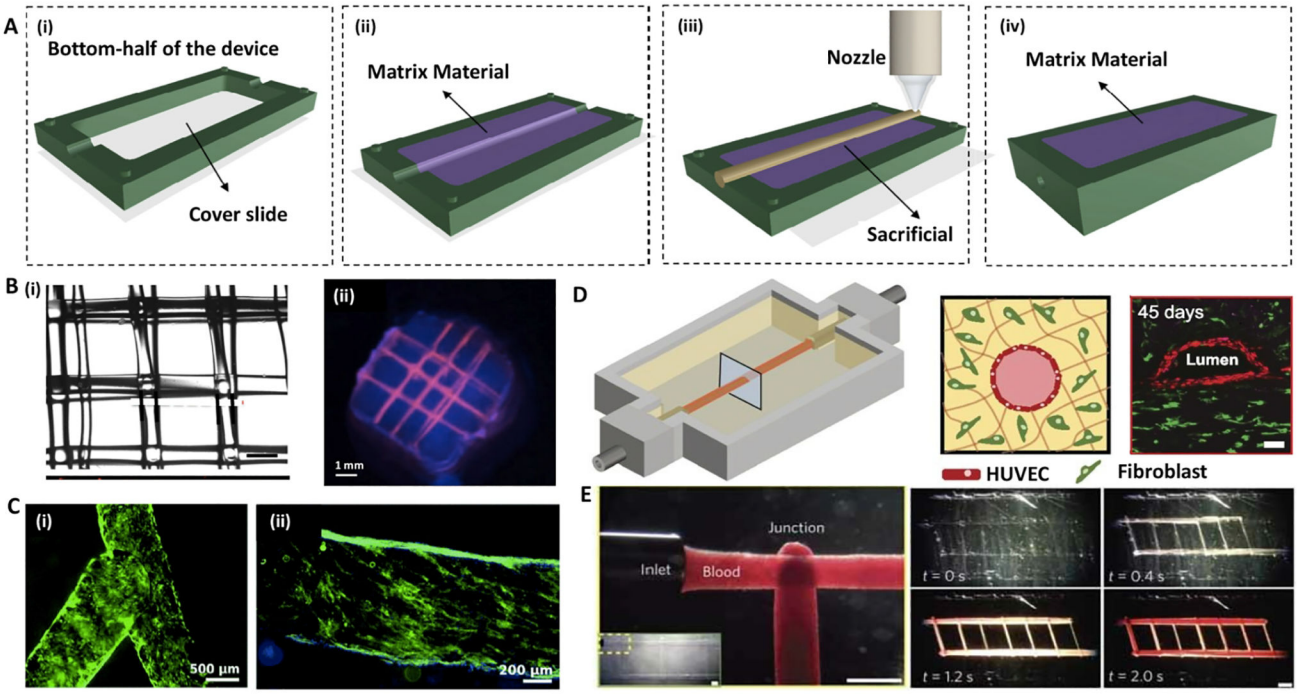

Fig. 2. Sacrificial extrusion-assisted bioprinting:

(A) Step-by-step display of a chip bioprinting: (i) the device is prepared with a bottom lid, (ii) imprinting a matrix material, (iii) bioprinting of the matrix material and (iv) liquefying the infusion bioink. (B) Agarose channels within GelMA hydrogel: (i) printed agarose template fibers, (ii) perfused fluorescent dye in the channel. (C) Pluronic F-127 channels within GelMA hydrogel: (i) bifurcated microchannels in the GelMA hydrogel, (ii) HUVECs CD31 (green) and nuclei (blue) staining. (D) Vascularized gelatin-based tissues, (left) HUVEC-lined vascular channel supporting a fibroblast-laden gelatin within a 3D perfusion chip (right) and long-term perfusion of HUVEC-lined (red) network supporting HNDF-laden (green) gelatin at day 45 (Scale bar: 100 µm). (E) Carbohydrate-glass lattice as the sacrificial element: patterned channels support positive pressure and pulsatile flow of human blood with inter-vessel junctions supporting branched fluid flow (left). Spiral flow patterns (right, 0.4 s; Scale bars: 1 mm for left and 2 mm for right). Reprinted with permission from references Datta *et al.* [37], Bertassoni *et al.* [33], Zhang *et al.* [44], Kolesky *et al.* [6] and Miller *et al.* [50].

Author Manuscript Author Manuscript Author Manuscript Author Manuscript

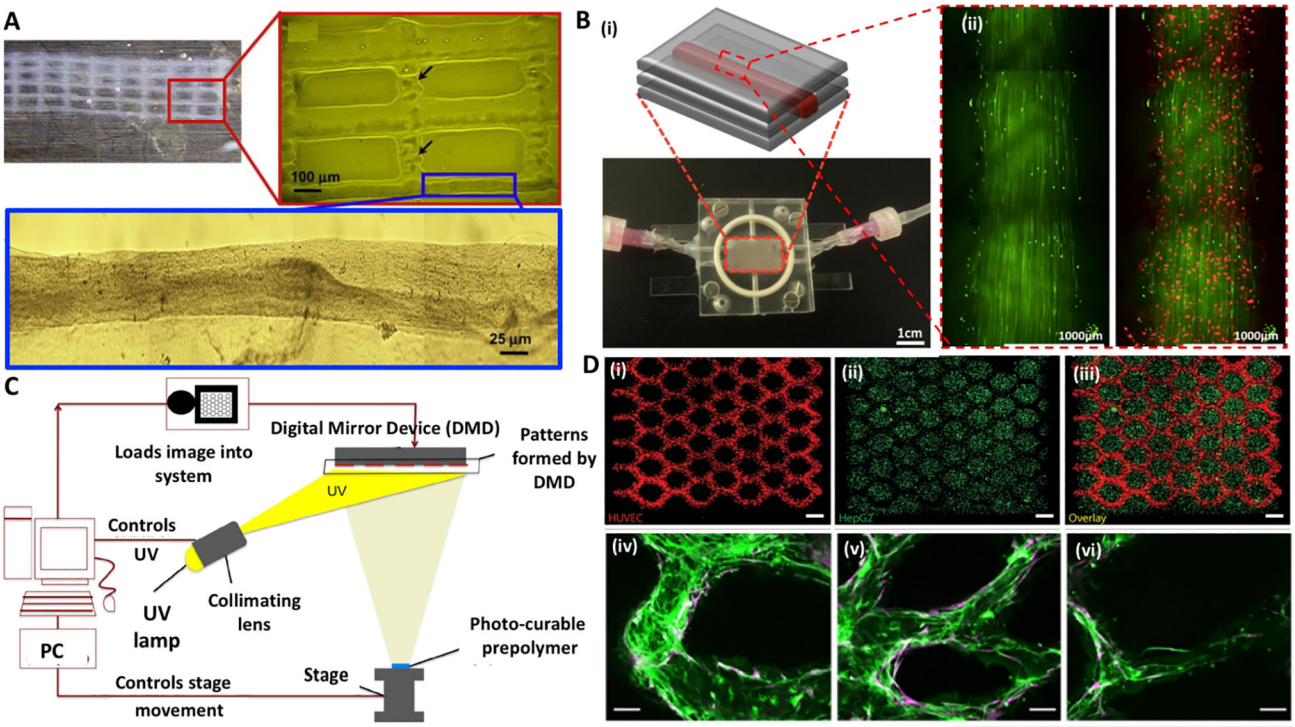

Fig. 3. Inkjet/Light-assisted strategies for 3D bioprinting:

(A) Inkjet-assisted printed fibrin scaffold, with minor deformations of the printed pattern (as indicated by arrows). (B) Perfusable microfluidic chip: (i) schematics of the setup, and (ii) HUVEC coated (red) long-term culture with human dermal fibroblasts support (red) after 45 second perfusion. (C) Schematic diagram of the DMD system: the UV light illuminates a programmable DMD chip, and is reflected down onto the photosensitive monomer solution. (D) Cell-laden DMD-printed constructs: (i) HUVECs are encapsulated in the channels and (ii) HepG2 are encapsulated in the surrounding area with (iii) overlay image (scale bars: 250 μm); (iv-vi) endothelial network formation after 1-week culture of the prevascularized tissue construct: (iv) showing HUVECs (Green, CD31) and (v) supportive MSCs (Purple, alpha-smooth muscle actin; scale bars: 100 μm). Reprinted with permission from references Cui *et al.* [57], Lee *et al.* [45], Huang *et al.* [58] and Zhu *et al.* [16].

Author Manuscript Author Manuscript Author Manuscript Author Manuscript

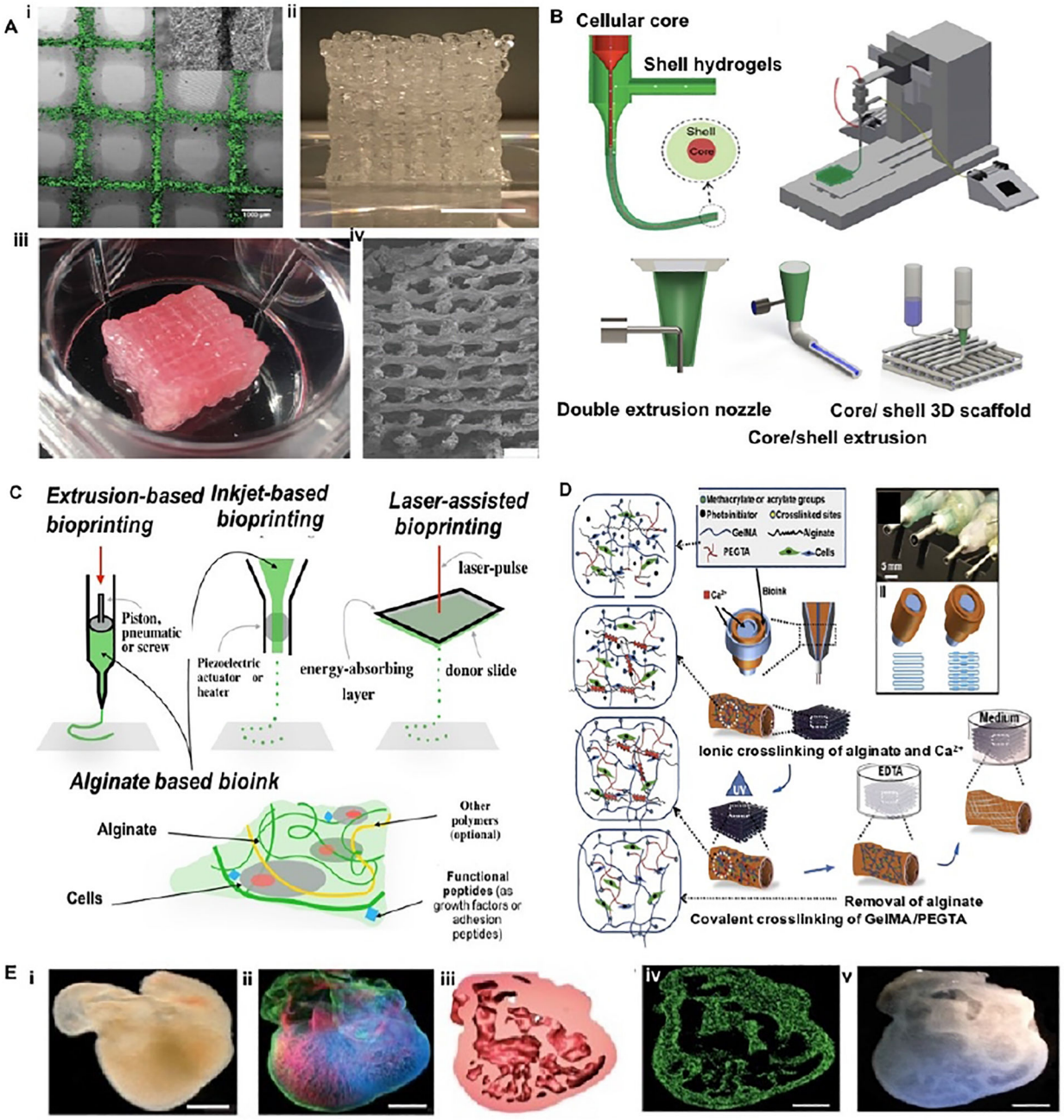

Fig. 4. Schematic of core/shell bioprinting:

(A) Printed lattices made by coaxial extrusion of alginate and gelatin hydrogels: (i) single layer of hybrid gel with fluorescently labelled cells in the core (Scale bar: 1 mm); (ii) 3D construct made by gelatin strands and cell-laden core/shell strands (Scale bar: 1 cm); (iii) structural integrity after the removal of gelatin; (iv) SEM image of the side profile showing interconnected pores (Scale bar: 1 mm). (B) 3D printing of core/shell cell-laden strands. (C) Three common bioprinting strategies using alginate-based assays. (D) Schematic diagram depicting two independent crosslinking procedures of the bioink, where PEGTA, alginate, and GelMA hydrogel are ionically and covalently crosslinked. (E) Bioprinting of embryonic

chick heart using alginate-based bioink: (i) typical embryonic chick heart (ii) stained for nuclei (blue), fibronectin (green), and F-actin (red); (iii) a cross-section of printed chicken heart; (iv) with fluorescent alginate (green); (v) optical microscopy image of the printed trabeculated embryonic chicken heart; (Scale bars: 1 mm). Reprinted with permission from references Mistry *et al.* [67], Akkineni *et al.* [75], Jia *et al.* [73], Axpe *et al.* [68], and Hilton *et al.* [40].

Author Manuscript Author Manuscript Author Manuscript Author Manuscript

Author Manuscript Author Manuscript Author Manuscript Author Manuscript

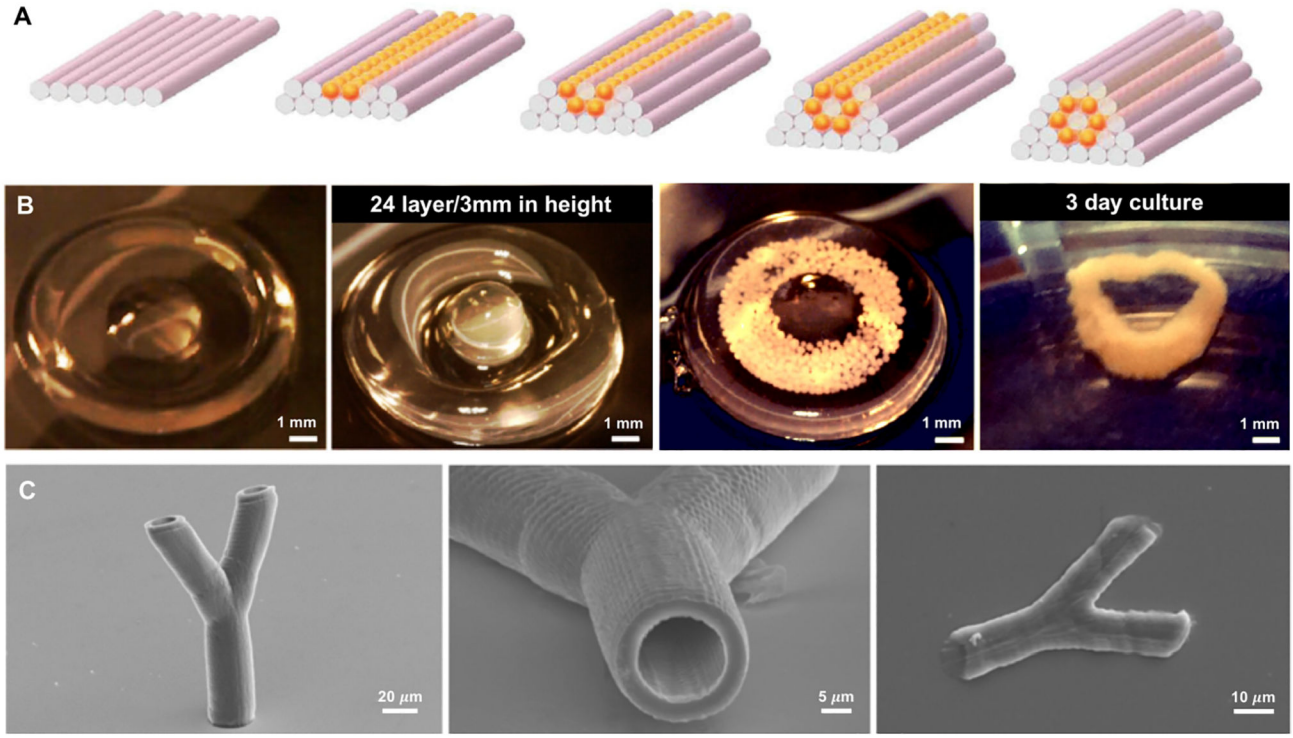

Fig. 5. Scaffold-free/freestanding bioprinting of shell constructs:

(A) Schematics showing vascular tissue engineering using scaffold-free bioprinting phase by phase, where agarose rods (pink) and similar multicellular spheroids (orange) were placed layer-by-layer. (B) Scaffold-free fabrication of bifurcated blood vessels using human skin fibroblast (HSF) spheroids that spheroids fuse into tissue after 6 days. (C) Scanning electron micrographs of tubular structure, by two-photon photocrosslinking of α, ω-poly-tetra-hydro-furan-ether-diacrylate resin, with a height of 160 μm (left), an inner diameter of 18 μm and wall thickness of 3 μm (middle), while smaller wall thicknesses around 1 μm collapsed (right). Reprinted with permission from references Datta *et al.* [37], Tan *et al.* [78] and Meyer *et al.* [83].

Author Manuscript Author Manuscript Author Manuscript Author Manuscript

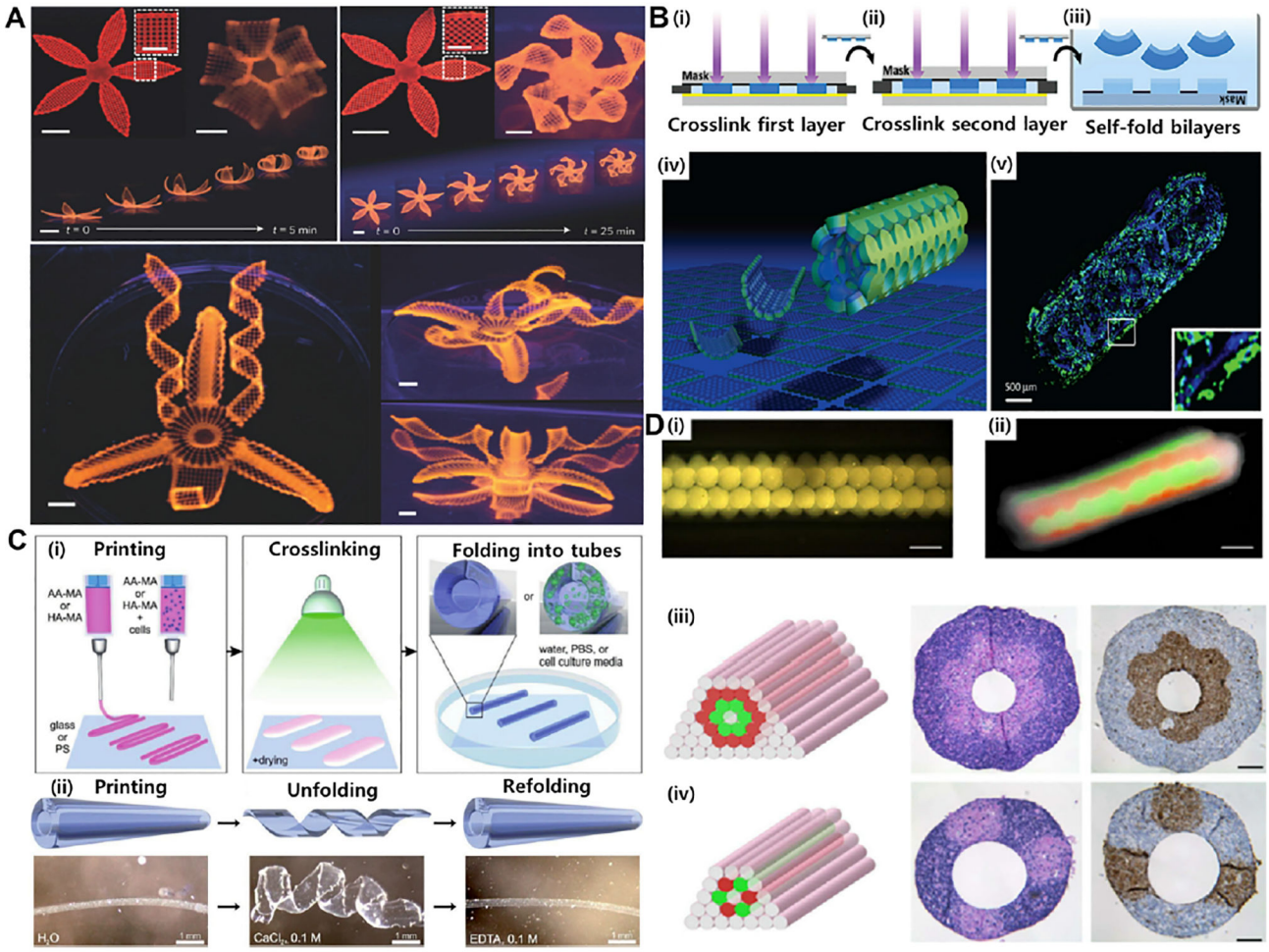

Fig. 6. Different approaches of 4D bioprinting:

(A) Different flower morphologies created by moisture responsive 4D printing using cellulose nanofiber acrylamide hydrogel (scale bars: 5 mm, inset: 2.5 mm). (B) Water responsive photopatterned PEG-based hydrogel bilayers: (i) the first layer printed, (ii) then added the second layer, and (iii) self-folded into curved hydrogels; (iv) schematic shown for multi-culture of cells in distinct layers of a self-folded hydrogel and (v) fluorescent micrographs indicting fibroblasts (blue: Hoechst) in the inner layer and fibroblasts (green: calcein) in the outer layer. (C) 4D printed self-folding tubes: (i) printing of methacryloyl alginate (AA-MA) or hyaluronic acid (HA-MA) followed by photocrosslinking with green light (530 nm) and instant folding into tubes upon immersion in water or cell culture media; (ii) self-folded methacryloyl alginate (schematics are at the upper panels and representative images are at the lower panels) that folded in water and unfolded by deswelling in calcium chloride, and then refolded in EDTA. (D) Bioprinting of vascular structures: (i) self-assembly of multicellular spheroids into (ii) tubular structures fused after one week showing red- and green-labeled cells; (iii, iv) two double-layered vascular models made of human umbilical vein smooth muscle cells (green) and skin fibroblasts (red) along with histology (center: H&E) and immunocytochemistry (right: smooth muscle α-actin in brown and Caspase-3 in brown) images (scale bars: 500 μm). Reprinted with permission from

Author Manuscript Author Manuscript Author Manuscript Author Manuscript

references Norotte *et al.* [81], Gladman *et al.* [93], Kirillova *et al.* [101], and Jamal *et al.* [99].

Author Manuscript Author Manuscript Author Manuscript Author Manuscript

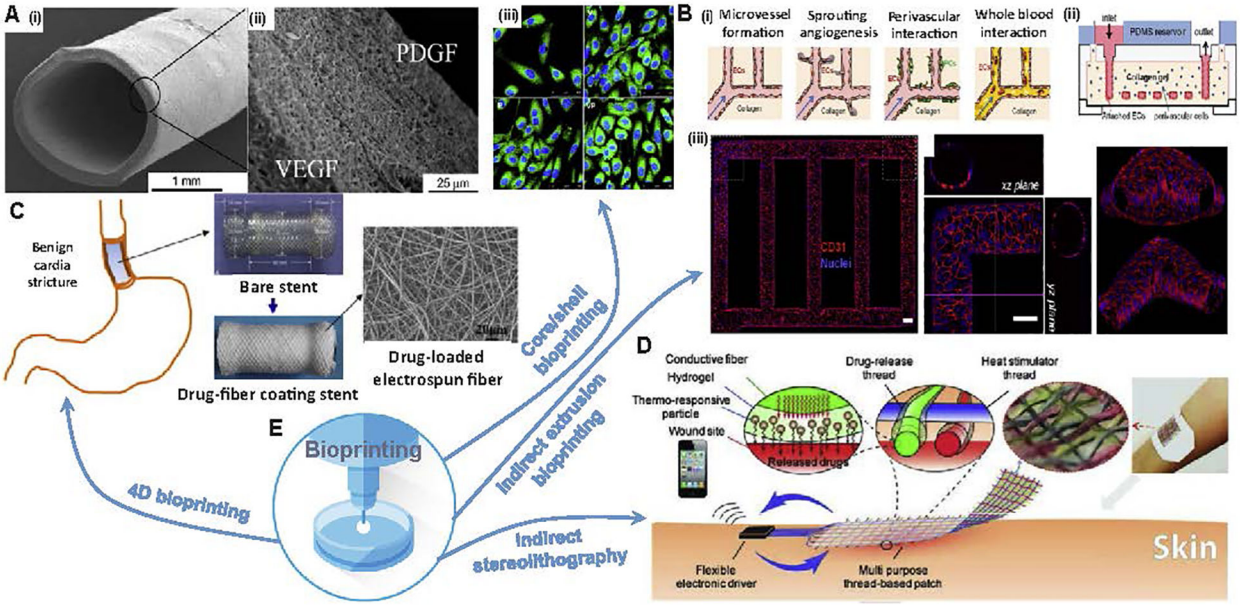

Fig. 7. Bioprinting solutions for drug carriers:

(A) Electrospun shell: i) SEM micrographs of 2.2-mm vascular graft, ii) cross section of the fibrous membrane loaded by vascular endothelial growth factor (VEGF) and platelet-derived growth factor (PDGF), iii) HUVECs stained with anti-CD31 antibody (FITC labeled CD31; Blue, DAPI stained nuclei) double-layered electrospun membranes loading single VEGF (top-right) or PDGF (bottom-left) or without any growth factor (top-left) loading dual VEGF and PDGF (bottom-right). (B) Microfluidic vessel networks: i) schematic cross-sectional view of a section of μVN illustrating (ii) morphology and barrier function of endothelium, iii) endothelial sprouting and perivascular association (Scale bar: 500 μm). (C) Biodegradable electrospun drug-fibers coated stent to inhibit inflammation and scar formation in benign esophageal structures. (D) Skin wound batch designed to release VEGF and other therapeutics into scar region. (E) Potential solutions through different bioprinting techniques. Reprinted with permission from references Zhang *et al.* [70], Zu *et al.* [122], Zheng *et al.* [123] and Mostafalu *et al.* [117].

Author Manuscript

Author Manuscript

Author Manuscript

Author Manuscript

Table 1.

Limitations of common bioprinting modalities for vascularized models

Parameter	Inkjet	Extrusion	Light
Fabrication speed	Medium	Low	High
Bioprinting resolution	100 – 300 μm	100 – 1000 μm	1 – 100 μm
Minimum vessel size	~ 200 μm	~ 100 μm	~ 1 μm
Cell viability	> 80%	< 80%	> 90%

Author Manuscript

Author Manuscript

Author Manuscript

Author Manuscript

Table 2.

Different Stimuli-Responsive 4D Bioprinting Techniques

Stimulus	Material	Mechanism	Refs
Water	Poly (ethylene glycol) (PEG)	Self-folding and swelling	[99]
	N,N-dimethylacrylamide, N-isopropyl-acrylamide and nanofibrillar cellulose	Biocompatible hydrogel matrices that readily swell in water	[93]
***p*H or temperature**	Lipid bilayers	Released by changing the pH or temperature	[90]
Temperature	Poly (acrylic acid)-poly (N-isopropylacrylamid), PAA–PNI PAM and ceramic powder Al_2O_3	Thermally induced tunable fluid-gel transition	[91]
	Alginate and poly (N-isopropylacrylamide)	Smart valve controlling water	[100]
Magnetic field	Polyurethane acrylate oligomers bioink and magnetized platelets	Magnetic force-induced deformation	[95]
Electrical field	Graphene-based biomaterials doped with gold/ carbon nanoparticles	Conducting electricity by intensity and/or direction	[94]
Light	Four-arm poly (ethylene glycol) tetrabicyclono nyne (PEG-tetra-BCN) and functionalized peptide	Photo-reversible patterning of full-length proteins within polymeric hydrogels	[92]